



Schwinger poles of the three-gluon vertex: symmetry and dynamics

A. C. Aguilar^{1,a}, M. N. Ferreira², B. M. Oliveira¹, J. Papavassiliou², L. R. Santos¹

¹ Institute of Physics “Gleb Wataghin”, University of Campinas-UNICAMP, Campinas, São Paulo 13083-859, Brazil

² Department of Theoretical Physics and IFIC, University of Valencia and CSIC, 46100 Valencia, Spain

Received: 3 July 2023 / Accepted: 19 September 2023 / Published online: 3 October 2023
© The Author(s) 2023

Abstract The implementation of the Schwinger mechanism endows gluons with a nonperturbative mass through the formation of special massless poles in the fundamental QCD vertices; due to their longitudinal character, these poles do not cause divergences in on-shell amplitudes, but induce detectable effects in the Green’s functions of the theory. Particularly important in this theoretical setup is the three-gluon vertex, whose pole content extends beyond the minimal structure required for the generation of a gluon mass. In the present work we analyze these additional pole patterns by means of two distinct, but ultimately equivalent, methods: the Slavnov–Taylor identity satisfied by the three-gluon vertex, and the nonlinear Schwinger–Dyson equation that governs the dynamical evolution of this vertex. Our analysis reveals that the Slavnov–Taylor identity imposes strict model-independent constraints on the associated residues, preventing them from vanishing. Approximate versions of these constraints are subsequently recovered from the Schwinger–Dyson equation, once the elements responsible for the activation of the Schwinger mechanism have been duly incorporated. The excellent coincidence between the two approaches exposes a profound connection between symmetry and dynamics, and serves as a nontrivial self-consistency test of this particular mass generating scenario.

1 Introduction

The emergence of a gluon mass [1–9] through the action of the Schwinger mechanism [10, 11] represents a prime example of how mass may emanate from interaction [12]. Indeed, the most appealing attribute of this mechanism is that it arises entirely from the underlying dynamics, without the slightest modification of the fundamental Lagrangian that

defines the theory, and, most importantly, leaving the local gauge symmetry intact [13, 14].

The cornerstone of the Schwinger mechanism is the non-perturbative formation of colored composite excitations with vanishing mass in the vertices of the theory [15–21], and especially in the three-gluon vertex, $\Pi_{\alpha\mu\nu}(q, r, p)$ [1, 9, 22–24]; for a variety of different approaches, see [25–34]. A special subset of these massless poles is transmitted to the gluon propagator, $\Delta(q)$, through the coupled dynamical equations of motion, i.e., Schwinger–Dyson equations (SDEs) [13, 14, 35–42], triggering finally its saturation at the origin, $\Delta^{-1}(0) = m^2 > 0$ [22–24, 43, 44].

Due to the special dynamical details governing their formation, the massless poles of the three-gluon vertex are *longitudinally coupled* [15–21], i.e., they correspond to tensorial structures of the general form q_α/q^2 , r_μ/r^2 , and p_ν/p^2 . As a result, they are not directly detectable in on-shell amplitudes, nor in lattice simulations of the corresponding correlation functions [45–62]; nonetheless, their effects are. Thus, in addition to causing the infrared saturation of the gluon propagator, the form factor $\mathbb{C}(q)$ associated with the pole induces a smoking-gun modification (“displacement”) to the Ward identity of the three-gluon vertex [14, 63–65]. Most importantly, the nonvanishing of $\mathbb{C}(q)$ has been unequivocally confirmed in [64], through the suitable combination of key inputs obtained from lattice QCD [57, 59, 66, 67].

This encouraging result motivates the further detailed scrutiny of the key features that the Schwinger mechanism induces in the three-gluon vertex. The main purpose of the present work is to carry out an extensive study of the full pole content of this vertex, determine the structure and role of the main components, and expose the delicate interplay between symmetry and dynamics that prompts their appearance. In that sense, our analysis provides a nontrivial confirmation of the internal consistency of this rather elaborate mass generating approach.

^a e-mail: aguilar@ifi.unicamp.br (corresponding author)

The dynamics of the pole formation are encoded in the nonlinear SDE that controls the evolution of $\Pi_{\alpha\mu\nu}(q, r, p)$. In their primordial manifestation, the massless poles arise as bound states of a particular kernel appearing in the skeleton expansion of this SDE [22, 22–24, 43, 44]; they are simple, of the type $1/q^2$, $1/r^2$, and $1/p^2$. When inserted into the SDE for $\Delta(q)$, only the pole in the direction of q is relevant for the generation of the gluon mass, which is expressed as an integral over the residue of this pole. However, due to the nonlinear nature of the vertex SDE, these “primary” poles give rise to additional “secondary” structures, corresponding to mixed double poles, of the general type $1/q^2 r^2$, $1/q^2 p^2$, $1/r^2 p^2$. In the Landau gauge, these poles are inert as far as mass generation is concerned; however, their presence is instrumental for the self-consistency of the entire approach, and in particular for preserving the fundamental relations that arise from the Becchi–Rouet–Stora–Tyutin (BRST) symmetry [68, 69] of the gauge-fixed Yang–Mills Lagrangian.

Indeed, the emergence of mixed poles finds its most compelling justification when the Slavnov–Taylor identity (STI) [70, 71] of the three-gluon vertex [72–75] is invoked. In its abelianized version, with the contributions of the ghost sector switched off, this STI states that $q^\alpha \Pi_{\alpha\mu\nu}(q, r, p) = P_{\mu\nu}(p)\Delta^{-1}(p) - P_{\mu\nu}(r)\Delta^{-1}(r)$, where $P_{\mu\nu}(q) = g_{\mu\nu} - q_\mu q_\nu / q^2$ is the standard projection operator. Let us now assume that the gluon propagator is infrared finite, i.e., $\Delta^{-1}(0) = m^2$. Then, in the limit $p^2 \rightarrow 0$ or $r^2 \rightarrow 0$, the r.h.s. of the STI displays longitudinally coupled massless poles, $p_\mu p_\nu / p^2$ and $r_\mu r_\nu / r^2$, whose residue is m^2 . Consequently, self-consistency requires that, in the same kinematic limits, the l.h.s. should exhibit the exact same pole structure, i.e., $\Pi_{\alpha\mu\nu}(q, r, p)$ must contain mixed poles, of the type $q_\alpha p_\mu p_\nu / q^2 p^2$ and $q_\alpha r_\mu r_\nu / q^2 r^2$, precisely as predicted by the vertex SDE.

The exact matching of pole contributions on both sides of the STI (with the ghost contributions duly restored) gives rise to a nontrivial relation, which expresses the form factors associated with the mixed poles in terms of components that appear on the r.h.s. of the STI. Quite interestingly, an approximate form of this special relation may be recovered from a truncated version of the vertex SDE. Moreover, an analogous construction reveals that the presence of a genuine triple mixed pole, of the type $1/q^2 p^2 r^2$ is *excluded* by both the STI and the SDE, being effectively reduced to a divergence weaker than a double mixed pole. These two exercises are especially illuminating, exposing a powerful synergy between symmetry and dynamics: whereas the STI (BRST symmetry) imposes relations that are valid regardless of the dynamical details, the SDE (nonlinear dynamics) reproduces them thanks to the distinct pole content induced by the Schwinger mechanism.

The article is organized as follows. In Sect. 2 we summarize the most salient features of the Schwinger mechanism

in QCD, commenting on some of its most recent advances. Then, in Sect. 3 we discuss in detail the pole structure induced to the three-gluon vertex when the Schwinger mechanism is activated, and in particular the appearance of mixed double and triple poles. In Sect. 4 we construct a tensor basis for the pole part of the vertex, which makes its Bose symmetry and longitudinal nature manifest, and will be used throughout this work. In Sect. 5 we consider the STI satisfied by the three-gluon vertex, and derive a crucial relation for a special kinematic limit of the form factor associated with the mixed double poles, denominated “residue function”. Then, in Sect. 6, we turn to the SDE of the three-gluon vertex, and derive, under certain simplifying assumptions, an approximate version of the aforementioned relation for the residue function. In continuation, in Sect. 7 we compute the residue function using as inputs all the components entering in that relation. Then, in Sect. 8, we demonstrate that both the STI and the detailed dynamics reduce substantially the strength of the triple mixed pole. Finally, in Sect. 9 we present our discussion and conclusions.

2 Schwinger mechanism in QCD: general concepts

In this section we present a brief overview of the implementation of the Schwinger mechanism in the context of a Yang–Mills theory; for further details, the reader is referred to two recent review articles [13, 14].

The natural starting point of the discussion is the gluon propagator, $\Delta_{\mu\nu}^{ab}(q) = -i\delta^{ab}\Delta_{\mu\nu}(q)$. In the *Landau gauge* that we employ throughout, $\Delta_{\mu\nu}(q)$ assumes the completely transverse form

$$\Delta_{\mu\nu}(q) = \Delta(q)P_{\mu\nu}(q), \quad P_{\mu\nu}(q) := g_{\mu\nu} - q_\mu q_\nu / q^2. \quad (2.1)$$

In the continuum, the momentum evolution of the function $\Delta(q)$ is determined by the corresponding SDE (Minkowski space),

$$\Delta^{-1}(q) = q^2 + i\Pi(q), \quad (2.2)$$

where $\Pi(q)$ is the scalar form factor of the gluon self-energy,

$$\Pi_{\mu\nu}(q) = \Pi(q)P_{\mu\nu}(q), \quad (2.3)$$

depicted diagrammatically in Fig. 1. Note that the fully-dressed vertices, Π , of the theory enter in the diagrams defining $\Pi_{\mu\nu}(q)$. In addition, it is convenient to introduce the dimensionless vacuum polarization, $\mathbf{\Pi}(q)$, defined as $\Pi(q) = q^2\mathbf{\Pi}(q)$, such that $\Delta^{-1}(q) = q^2[1 + \mathbf{\Pi}(q)]$.

The basic premise underpinning the Schwinger mechanism may be expressed as follows: if $\mathbf{\Pi}(q)$ develops a pole

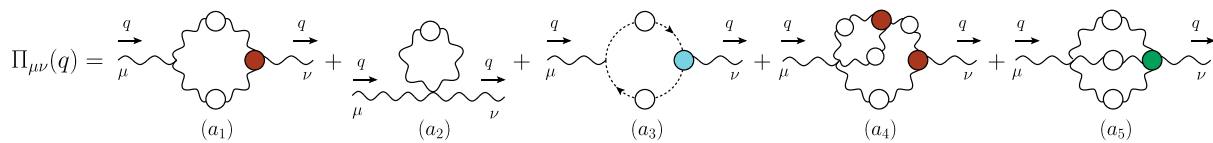


Fig. 1 The diagrammatic representation of the gluon self-energy. The fully-dressed three-gluon, ghost–gluon, and four-gluon vertices are depicted as red, blue, and green circles, respectively. The special analytic structure of these vertices induces the poles required for the activation of the Schwinger mechanism

with positive residue at $q^2 = 0$ (*massless pole*), the gauge boson (gluon) acquires a mass, even if the symmetries of the theory do not admit a mass term at the level of the fundamental Lagrangian [10, 11]. In particular, the appearance of such a pole triggers the basic sequence (Euclidean space)

$$\begin{aligned} \lim_{q \rightarrow 0} \Pi(q) = m^2/q^2 &\implies \lim_{q \rightarrow 0} \Delta^{-1}(q) \\ &= \lim_{q \rightarrow 0} (q^2 + m^2) \implies \Delta^{-1}(0) = m^2, \end{aligned} \tag{2.4}$$

where the residue of the pole acts as the effective squared gluon mass, m^2 .

The pivotal result captured by Eq. (2.4) invites the natural question of what makes $\Pi(q)$ exhibit massless poles in the first place. In the case of four-dimensional Yang–Mills theories, such as QCD, the answer to this question is that these poles are transmitted to $\Pi(q)$ by the fully-dressed vertices that appear in the diagrammatic expansion of the gluon self-energy [1, 9, 13, 14, 76], see Fig. 1. The poles of the vertices are produced dynamically, when elementary fields (e.g., two gluons, two ghosts, or three gluons) merge to create composite colored scalars with vanishing masses [15–21]. These processes are controlled by appropriate bound-state equations, analogous to the standard Bethe–Salpeter equations (BSEs) [77, 78]; they arise as special kinematic limits ($q \rightarrow 0$) of the SDEs governing the various vertices [22, 24, 43, 44]. The residues of the vertices are functions of the remaining kinematic variables; when convoluted with the rest of the components comprising the gluon SDE, they account for the final residue, m^2 , that one identifies as the squared gluon mass in Eq. (2.4) [22, 24, 43, 44].

To elucidate how a contribution to the total gluon mass emerges from diagram (a₁) in Fig. 1, consider the three-gluon vertex $\Pi_{\alpha\mu\nu}^{abc}(q, r, p) = g f^{abc} \Gamma_{\alpha\mu\nu}(q, r, p)$, where g is the gauge coupling, f^{abc} the structure constants of the SU(3) gauge group, and $q + r + p = 0$. The formation of the poles in the three-gluon vertex may be described by separating $\Gamma_{\alpha\mu\nu}(q, r, p)$ in two distinct pieces,

$$\Gamma_{\alpha\mu\nu}(q, r, p) = \Gamma_{\alpha\mu\nu}(q, r, p) + V_{\alpha\mu\nu}(q, r, p), \tag{2.5}$$

where $\Gamma_{\alpha\mu\nu}(q, r, p)$ represents the pole-free component, while $V_{\alpha\mu\nu}(q, r, p)$, whose origin is purely non-perturbative, contains all pole-related contributions. As we will discuss in detail in the next sections, the composition of $V_{\alpha\mu\nu}(q, r, p)$

is rather elaborate; however, for the purposes of creating a mass for the gluon propagator in the Landau gauge, only a minimal structure of $V_{\alpha\mu\nu}(q, r, p)$ is required, namely¹

$$V_{\alpha\mu\nu}(q, r, p) = \frac{q_\alpha}{q^2} g_{\mu\nu} V_1(q, r, p) + \dots, \tag{2.6}$$

where all omitted terms drop out when $V_{\alpha\mu\nu}(q, r, p)$ is inserted in diagrams (a₁).

A detailed analysis reveals that [79]

$$V_1(0, r, -r) = 0; \tag{2.7}$$

therefore, the Taylor expansion of $V_1(q, r, p)$ around $q = 0$ yields

$$\begin{aligned} \lim_{q \rightarrow 0} V_1(q, r, p) &= 2(q \cdot r) \mathbb{C}(r) + \mathcal{O}(q^2), \\ \mathbb{C}(r) &:= \left[\frac{\partial V_1(q, r, p)}{\partial p^2} \right]_{q=0}. \end{aligned} \tag{2.8}$$

With the aid of Eq. (2.8), and after the extraction of the appropriate tensorial structure, the integral associated with the diagram (a₁) yields

$$m^2_{(a_1)} = -\Delta_{(a_1)}^{-1}(0) = 3\lambda Z_3 \int_k k^2 \Delta^2(k) \mathbb{C}(k), \tag{2.9}$$

with

$$\lambda := i g^2 C_A / 2, \tag{2.10}$$

where C_A is the Casimir eigenvalue of the adjoint representation [N for SU(N)]. In the above formula, Z_3 stands for the renormalization constant of the three-gluon vertex, and we denote by

$$\int_k := \frac{1}{(2\pi)^4} \int d^4k \tag{2.11}$$

the integration over virtual momenta; the use of a symmetry-preserving regularization scheme is implicitly assumed.

¹ In previous works [43, 44, 63, 64, 79], $V_1(q, r, p)$ has been denoted as $C_1(q, r, p)$.

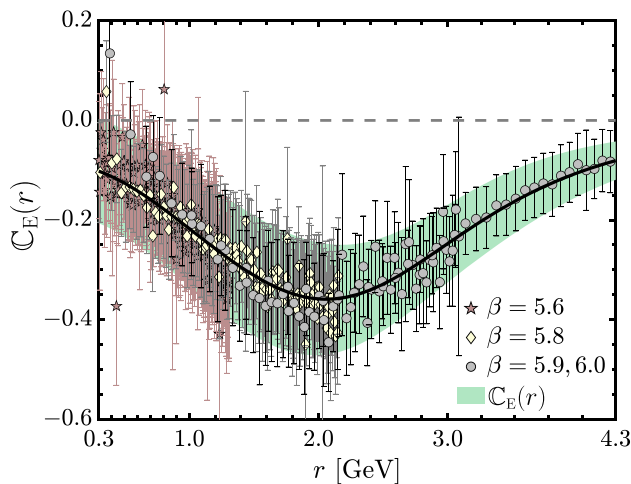


Fig. 2 The displacement function, $C_E(r)$, obtained from [64,65]

We next use standard rules (see eg [63]) to rewrite Eq. (2.9) in Euclidean space; note, in particular, that $m^2 = \Delta_E(0)$. Then, using hyperspherical coordinates, we obtain

$$m_{(a_1)}^2 = \frac{3\alpha_s C_A Z_3}{8\pi} \int_0^\infty dy y^2 \Delta_E^2(y) |C_E(y)|, \quad (2.12)$$

with $\alpha_s := g^2/(4\pi)$ and $y := k_E^2$. Evidently, m^2 depends on the renormalization point, μ ; in particular, $m = 348$ MeV for $\mu = 4.3$ GeV [34,67]².

We emphasize that $C_E(q)$, in addition to providing the gluon mass through Eq. (2.12) and its two-loop extension, plays a central role in this entire construction due to its dual nature. In particular:

- (i) $C_E(r)$ is the *BS amplitude* describing the formation of gluon–gluon *colored* composite bound states;
- (ii) $C_E(r)$ leads to a characteristic displacement of the WI satisfied by the pole-free part of the three-gluon vertex; for that reason, $C_E(r)$ is called “*displacement function*”. This predicted displacement has been confirmed by combining judiciously the results of several lattice simulations [64,65]; as shown in Fig. 2, the result for $C_E(r)$ is clearly nonvanishing.

3 Schwinger poles of the three-gluon vertex

In this section we elaborate on the pole content of the three-gluon vertex, which arises as a consequence of the activation of the Schwinger mechanism. Our analysis relies on the bound-state interpretation of the poles associated with the Schwinger mechanism (see e.g., [22,43,44,63,64,79]),

² A renormalization-group-invariant gluonic mass scale of about half the proton mass has been obtained from the process-independent QCD effective charge [80,81].

making extensive use of the diagrammatic structure of the SDE of the three-gluon vertex.

The dynamics of $\Pi_{\alpha\mu\nu}(q, r, p)$ are determined by the SDE shown in panel (A) of Fig. 3. Following the standard way of writing the SDE of a vertex, a particular gluon leg of $\Pi_{\alpha\mu\nu}(q, r, p)$ is singled out (in this case the leg carrying momentum q), and is connected to the various multiparticle kernels through all elementary vertices of the theory. The remaining two legs (with momenta r and p) are attached to the multiparticle kernels through fully-dressed vertices. Note that the full SDE is Bose-symmetric, albeit not manifestly so³; in order to expose its Bose symmetry, the detailed skeleton expansion of the kernels must be taken into account.

The seed of the Schwinger mechanism may be traced inside the four-particle kernel appearing in the top panel of Fig. 3. It is triggered by the emergence of a colored scalar excitation, formed as a bound state of a pair of gluons, as shown pictorially in the bottom panel of Fig. 3; note that the propagator of the composite scalar is given by $i\delta^{ab}/q^2$. The resulting scalar-gluon–gluon interaction is described by the tensor denoted by $B_{\mu\nu}(q, r, p)$ in the bottom panel of Fig. 3. The dynamics of $B_{\mu\nu}(q, r, p)$ is determined by solving the linear homogeneous BSE, which arises as the limit $q \rightarrow 0$ of the SDE for $\Pi_{\alpha\mu\nu}(q, r, p)$ is taken. The nontrivial solution that one obtains corresponds to the “BS amplitude” for the formation of a massless scalar out of two gluons. As explained in detail in [13], the BS amplitude coincides, up to an overall scaling factor, with the displacement function $C(q)$.

When the upper part of the four-gluon kernel (legs with $k + q$ and $-k$) is connected to the external gluon (with momentum q) in order to form the three-gluon vertex, as shown in the bottom panel of Fig. 3, the part that contains the composite scalar gives rise to the transition amplitude $I_\alpha(q)$, defined in Fig. 4. Lorentz invariance imposes that $I_\alpha(q) = I(q) q_\alpha$, where $I(q)$ is a scalar function, whose role and properties have been discussed in detail in [13,24]; note, in particular, the exact relation $m^2 = g^2 I^2(0)$. As a consequence, the massless poles are *longitudinally coupled* [15,17–20], giving rise to tensorial structures of the general form q_α/q^2 , r_μ/r^2 , and p_ν/p^2 . Therefore, the pole part, $V_{\alpha\mu\nu}(q, r, p)$, satisfies the important relation

$$P_{\alpha'}^\alpha(q) P_{\mu'}^\mu(r) P_{\nu'}^\nu(p) V_{\alpha\mu\nu}(q, r, p) = 0. \quad (3.1)$$

Note, in addition, that when $V_{\alpha\mu\nu}(q, r, p)$ is contracted by two transverse projectors, only the poles in the uncontracted

³ Within the n PI effective action formalism, the resulting SDE for the three-gluon vertex is manifestly Bose-symmetric with respect to all of its three legs [82–87].

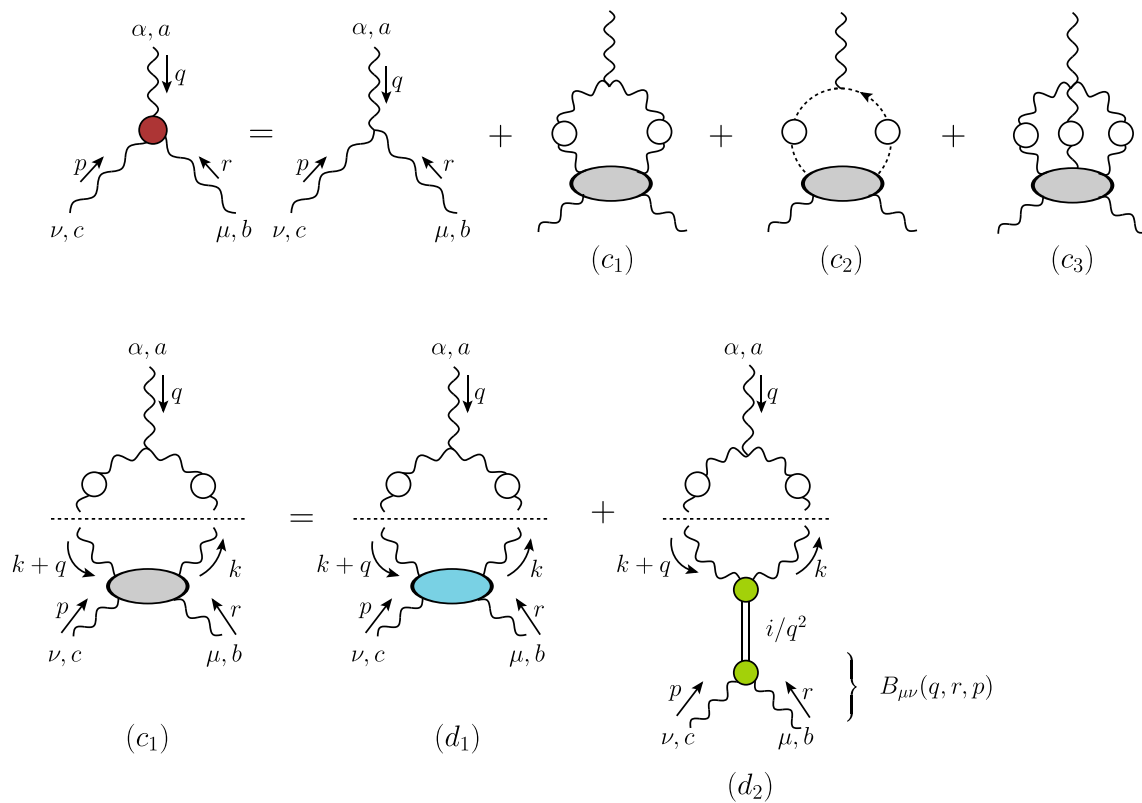


Fig. 3 Top: skeleton expansion of the three-gluon vertex. The gray ellipses denote multi-particle kernels, which are one-particle irreducible with respect to the q -channel. Bottom: decomposition of the kernel of diagram (c1) into a term with no poles in the q channel, denoted by (d1) (blue ellipse), and a term that contains a massless bound state,

with propagator i/q^2 , denoted by (d2). For the purpose of clearer visualization of the various structures, the components of the four-gluon kernel are separated from the corresponding vertex graphs by dotted horizontal lines

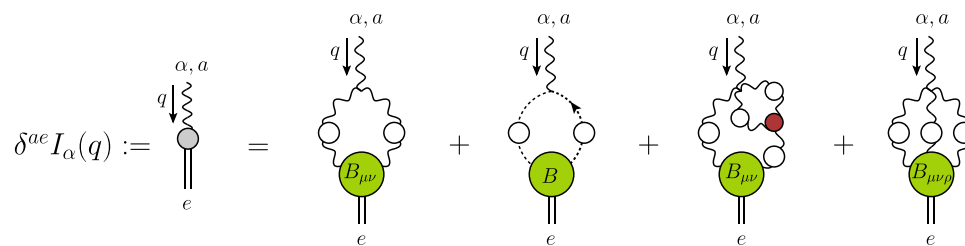


Fig. 4 Definition of the scalar-gluon transition amplitude, $I_\alpha(q)$. The green circles represent the so-called “proper vertex functions” or “bound state wave functions” [16]. In particular, the $B_{\mu\nu}$, first introduced in

Fig. 3, describes the effective interaction between a composite scalar and two gluons, while B and $B_{\mu\nu\rho}$ describe the interaction of a composite scalar with a ghost-antighost pair and three gluons, respectively

channel survive, e.g.⁴,

$$P_{\mu'}^\mu(r) P_{\nu'}^\nu(p) V_{\alpha\mu\nu}(q, r, p) = \text{only poles in } q^2. \quad (3.2)$$

The nonlinear nature of the SDE makes $V_{\alpha\mu\nu}(q, r, p)$ contain mixed poles, of the type $q_\alpha r_\mu / q^2 r^2$, etc. In the Landau

gauge, these additional terms do not affect the gluon mass, which only depends on the residue of the single pole that coincides with the external momentum of the gluon SDE (q in the conventions of Fig. 1). Nonetheless, this type of pole is crucial for maintaining gauge invariance, by balancing properly the STI satisfied by $\Gamma_{\alpha\mu\nu}(q, r, p)$. In order to appreciate how such terms arise, we make the following two key observations.

⁴ In the language of Eq. (4.4), $P_{\mu'}^\mu(r) P_{\nu'}^\nu(p) V_{\alpha\mu\nu}(q, r, p) = \frac{q_\alpha}{q^2} P_{\mu'}^\mu(r) P_{\nu'}^\nu(p) [V_1 g_{\mu\nu} + V_2 p_\mu r_\nu]$.

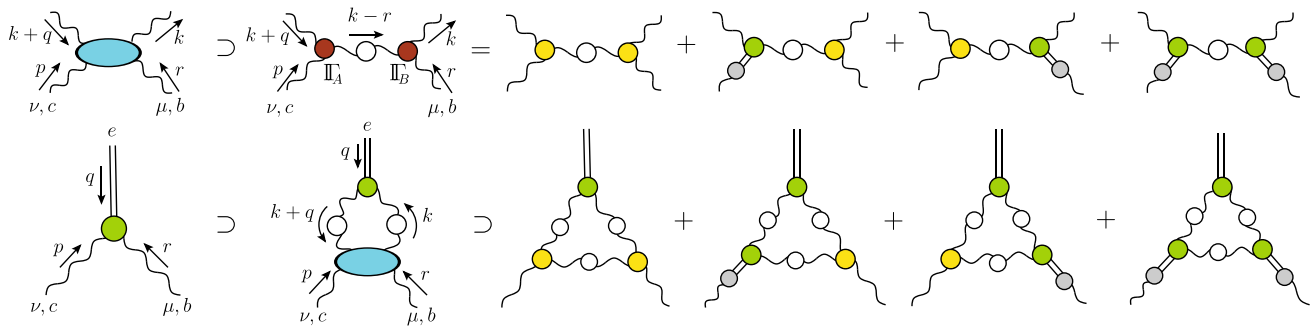


Fig. 5 Top: one-gluon exchange form of the blue kernel introduced in Fig. 3, and its subsequent decomposition into pole-free part (yellow vertices) and terms containing poles in r and p . Bottom: decomposition of the scalar-gluon-gluon interaction, $B_{\mu\nu}(q, r, p)$, defined in of Fig. 3, into pole-free and pole terms

(i) To begin with, the part of the vertex with no poles in the channel q , contains poles in the other two (r and p). This is because the kernel associated with this part (blue ellipse in Fig. 3) contains fully dressed vertices, as indicated schematically in the top panel of Fig. 5, for the case of the “one-gluon exchange” approximation. Denoting by $\Pi_A := \Pi(p, k + q, r - k)$ and $\Pi_B := \Pi(r, k - r, -k)$, as indicated in Fig. 5, the contribution to the (d_1) of Fig. 3 may be schematically written as

$$(d_1) \sim \int_k \Gamma^{(0)} \Delta \Pi_A \Delta \Pi_B \Delta \sim \int_k \Gamma^{(0)} \Delta (\Gamma_A + V_A) \Delta (\Gamma_B + V_B) \Delta, \tag{3.3}$$

where

$$\Gamma_{\alpha\mu\nu}^{(0)}(q, r, p) = (q - r)_\nu g_{\alpha\mu} + (r - p)_\alpha g_{\mu\nu} + (p - q)_\mu g_{\nu\alpha}, \tag{3.4}$$

is the tree-level expression of the three-gluon vertex.

Then, using Eq. (2.5), and noting that the vertices V_A and V_B furnish poles only in the external momenta p , and r , respectively, since poles in all other directions are annihilated by the Landau gauge propagators [see Eq. (3.2)], one obtains

$$(d_1) \sim \underbrace{\int_k \Gamma^{(0)} \Delta \Gamma_A \Delta \Gamma_B \Delta}_{\text{no pole}} + \underbrace{\int_k \Gamma^{(0)} \Delta V_A \Delta \Gamma_B \Delta}_{\text{pole in } p^2} + \underbrace{\int_k \Gamma^{(0)} \Delta \Gamma_A \Delta V_B \Delta}_{\text{pole in } r^2} + \underbrace{\int_k \Gamma^{(0)} \Delta V_A \Delta V_B \Delta}_{\text{poles in } r^2, p^2}. \tag{3.5}$$

(ii) Furthermore, the same kernel appears in the part of the vertex describing the pole in the q -channel. Thus, as indicated in the bottom panel of Fig. 5, one obtains contributions of the type

$$(d_2) \sim \int_k V \Delta \Pi_A \Delta \Pi_B \Delta \sim \int_k V \Delta (\Gamma_A + V_A) \Delta (\Gamma_B + V_B) \Delta, \tag{3.6}$$

giving rise to

$$(d_2) \sim \underbrace{\int_k V \Delta \Gamma_A \Delta \Gamma_B \Delta}_{\text{pole in } q^2} + \underbrace{\int_k V \Delta V_A \Delta \Gamma_B \Delta}_{\text{poles in } q^2, p^2} + \underbrace{\int_k V \Delta \Gamma_A \Delta V_B \Delta}_{\text{poles in } q^2, r^2} + \underbrace{\int_k V \Delta V_A \Delta V_B \Delta}_{\text{poles in } q^2, r^2, p^2}. \tag{3.7}$$

The main conclusion of the analysis presented in this section is summarized in Fig. 6, where Eq. (2.5) is represented pictorially. In particular, the component $V_{\alpha\mu\nu}(q, r, p)$ is comprised by single poles, mixed double poles, and mixed triple pole, depending on the number of gluon-scalar transition amplitudes (grey circles) contained in them. The three types of effective amplitudes, $T_{\mu\nu}(q, r, p)$, $T_\mu(q, r, p)$, and $T(q, r, p)$ (white circles) are completely pole-free; see also Eq. (4.9).

We end this section with two final comments.

First, as we will demonstrate in Sect. 8, the triple mixed pole is not genuine; its strength is reduced due to requirements imposed by the self-consistency of the vertex STI, or, at the diagrammatic level, by virtue of Eq. (2.8).

Second, the validity of Eq. (3.1), which, in the bound-state formulation of the Schwinger mechanism arises naturally, guarantees that the lattice “observables” of the general form

$$L(q, r, p) = \frac{\lambda_{\alpha\mu\nu}(q, r, p) P_{\alpha\alpha'}(q) P_{\mu\mu'}(r) P_{\nu\nu'}(p) \Pi^{\alpha'\mu'\nu'}(q, r, p)}{\lambda_{\alpha\mu\nu}(q, r, p) P_{\alpha\alpha'}(q) P_{\mu\mu'}(r) P_{\nu\nu'}(p) \Gamma_0^{\alpha'\mu'\nu'}(q, r, p)}, \tag{3.8}$$

where the $\lambda_{\alpha\mu\nu}(q, r, p)$ are appropriate projectors, are completely pole-free. Indeed, all lattice results obtained thus far show no trace of pole divergences [49–60, 88, 89].

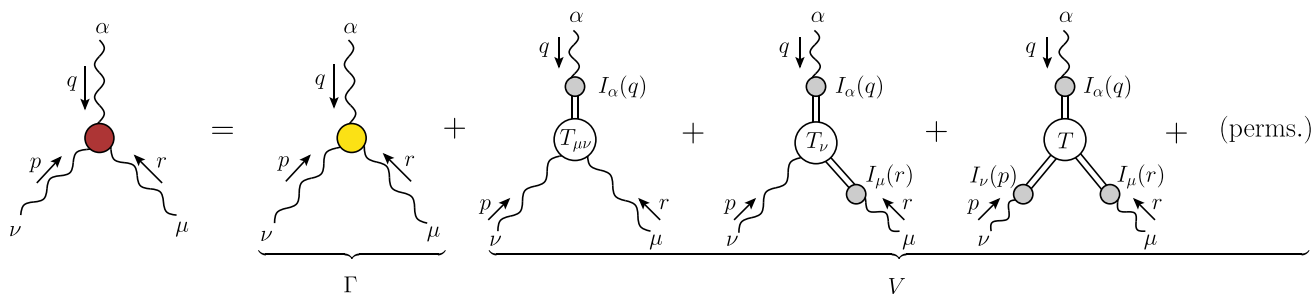


Fig. 6 The general structure of the three-gluon vertex after the activation of the Schwinger mechanism. Note, in particular, that the term $V_{\alpha\mu\nu}(q, r, p)$ contains single poles, such as q_α/q^2 , as well as mixed

poles of the forms $q_\alpha r_\mu/q^2 r^2$ and $q_\alpha r_\mu p_\nu/q^2 r^2 p^2$. The term “(perms)” denotes the permutations of the external legs that lead to a Bose-symmetric $V_{\alpha\mu\nu}(q, r, p)$

4 A purely longitudinal basis

In this section we introduce an appropriate basis for describing the special component $V^{\alpha\mu\nu}(q, r, p)$, which, due to the condition Eq. (3.1), is strictly longitudinal.

As is well known, the most general Lorentz decomposition of the three-gluon vertex is comprised of 14 independent tensors. However, the strict longitudinality condition of Eq. (3.1) imposes 4 constraints on the form factors of $V^{\alpha\mu\nu}(q, r, p)$. As a result, $V^{\alpha\mu\nu}(q, r, p)$ can be decomposed in a basis comprised of 10 tensors, denoted by $v_i^{\alpha\mu\nu}(q, r, p)$, accompanied by the associated form factors, denoted by $\mathbb{V}_i(q, r, p)$, i.e.,

$$V^{\alpha\mu\nu}(q, r, p) = \sum_{i=1}^{10} \mathbb{V}_i(q, r, p) v_i^{\alpha\mu\nu}(q, r, p), \tag{4.1}$$

where

$$\begin{aligned} v_1^{\alpha\mu\nu} &= q^\alpha g^{\mu\nu}, & v_2^{\alpha\mu\nu} &= q^\alpha p^\mu r^\nu, & v_3^{\alpha\mu\nu} &= r^\mu g^{\nu\alpha}, \\ v_4^{\alpha\mu\nu} &= r^\mu q^\nu p^\alpha, & v_5^{\alpha\mu\nu} &= p^\nu g^{\alpha\mu}, & v_6^{\alpha\mu\nu} &= p^\nu r^\alpha q^\mu, \\ v_7^{\alpha\mu\nu} &= q^\alpha r^\mu (q-r)^\nu, & v_8^{\alpha\mu\nu} &= r^\mu p^\nu (r-p)^\alpha, & v_9^{\alpha\mu\nu} &= p^\nu q^\alpha (p-q)^\mu, \\ v_{10}^{\alpha\mu\nu} &= q^\alpha r^\mu p^\nu. \end{aligned} \tag{4.2}$$

Note that these tensors form three distinct groups, depending on the number of momenta to which they are longitudinal: the $v_i^{\alpha\mu\nu}$ with $i = 1, \dots, 6$ are longitudinal to a single momentum, those with $i = 7, \dots, 9$ to two, while $v_{10}^{\alpha\mu\nu}$ is longitudinal to all three momenta.

Now, following the bound state interpretation, each form factor \mathbb{V}_i can have massless poles in each of the channels to which the corresponding tensor, $v_i^{\alpha\mu\nu}$, is longitudinal. In particular, exhibiting the poles explicitly, we have

$$\begin{aligned} \mathbb{V}_1 &= \frac{V_1}{q^2}; & \mathbb{V}_3 &= \frac{V_3}{r^2}; & \mathbb{V}_5 &= \frac{V_5}{p^2}; & \mathbb{V}_7 &= \frac{V_7}{q^2 r^2}; \\ \mathbb{V}_9 &= \frac{V_9}{p^2 q^2}; \end{aligned}$$

$$\begin{aligned} \mathbb{V}_2 &= \frac{V_2}{q^2}; & \mathbb{V}_4 &= \frac{V_4}{r^2}; & \mathbb{V}_6 &= \frac{V_6}{p^2}; & \mathbb{V}_8 &= \frac{V_8}{r^2 p^2}; \\ \mathbb{V}_{10} &= \frac{V_{10}}{q^2 r^2 p^2}, \end{aligned} \tag{4.3}$$

where the $V_i \equiv V_i(q, r, p)$ are regular functions, which, in the appropriate limits, capture the corresponding pole residues.

With the above definitions, $V_{\alpha\mu\nu}(q, r, p)$ can be recast in the form

$$\begin{aligned} V_{\alpha\mu\nu}(q, r, p) &= \frac{q_\alpha}{q^2} (g_{\mu\nu} V_1 + p_\mu r_\nu V_2) \\ &+ \frac{r_\mu}{r^2} (g_{\alpha\nu} V_3 + q_\nu p_\alpha V_4) \\ &+ \frac{p_\nu}{p^2} (g_{\alpha\mu} V_5 + r_\alpha q_\mu V_6) \\ &+ \frac{q_\alpha r_\mu}{q^2 r^2} (q-r)_\nu V_7 + \frac{r_\mu p_\nu}{r^2 p^2} (r-p)_\alpha V_8 \\ &+ \frac{p_\nu q_\alpha}{p^2 q^2} (p-q)_\mu V_9 + \frac{q_\alpha r_\mu p_\nu}{q^2 r^2 p^2} V_{10}. \end{aligned} \tag{4.4}$$

It is clear from the diagrammatic representation of Fig. 6, that $V_{\alpha\mu\nu}(q, r, p)$ is Bose-symmetric. Consequently, and given that the color factor f^{abc} has been factored out, we have that

$$V_{\alpha\mu\nu}(q, r, p) = -V_{\mu\alpha\nu}(r, q, p) = -V_{\nu\mu\alpha}(p, r, q). \tag{4.5}$$

Then, from Eqs. (4.4) and (4.5) follows that the form factors $V_i(q, r, p)$ satisfy the following symmetry relations

$$\begin{aligned} V_{1,2}(q, r, p) &= -V_{1,2}(q, p, r), & V_7(q, r, p) &= V_7(r, q, p), \\ V_{3,4}(q, r, p) &= -V_{3,4}(p, r, q), & V_8(q, r, p) &= V_8(q, p, r), \\ V_{5,6}(q, r, p) &= -V_{5,6}(r, q, p), & V_9(q, r, p) &= V_9(p, r, q), \end{aligned} \tag{4.6}$$

with $V_{10}(q, r, p)$ being totally anti-symmetric. In addition, some form factors are related to each other by the cyclic

permutations of their arguments, namely

$$\begin{aligned} V_{3,4}(q, r, p) &= V_{1,2}(r, p, q), & V_8(q, r, p) &= V_7(r, p, q), \\ V_{5,6}(q, r, p) &= V_{1,2}(p, q, r), & V_9(q, r, p) &= V_7(p, q, r). \end{aligned} \tag{4.7}$$

In the limit $q \rightarrow 0$, we obtain from Eq. (4.6) the relations

$$\begin{aligned} V_1(0, r, -r) &= V_3(r, 0, -r) = V_5(r, -r, 0) = 0, \\ V_2(0, r, -r) &= V_4(r, 0, -r) = V_6(r, -r, 0) = 0, \\ V_{10}(0, r, -r) &= V_{10}(r, 0, -r) = V_{10}(r, -r, 0) = 0. \end{aligned} \tag{4.8}$$

The relations derived above will be employed in the analysis presented in the following sections.

Finally, it is instructive to make contact between the form of the vertex $V_{\alpha\mu\nu}(q, p, r)$ given in Eq. (4.4) and the pictorial representation of the same vertex, depicted in Fig. 6. In particular, the effective amplitudes $T_{\mu\nu}$, T_μ , and T may be expressed in terms of the form factors V_i through the direct matching of the various tensorial structures, namely

$$\begin{aligned} I(q)T_{\mu\nu}(q, r, p) &= -i \left[g_{\mu\nu}V_1(q, r, p) \right. \\ &\quad \left. + p_\mu r_\nu V_2(q, r, p) \right], \\ I(q)I(r)T_\nu(q, r, p) &= (r - q)_\nu V_7(q, r, p), \\ I(q)I(r)I(p)T(q, r, p) &= iV_{10}(q, r, p). \end{aligned} \tag{4.9}$$

We conclude this discussion with some remarks regarding the basis given by Eq. (4.2). The 14 tensors required for the full description of $\Pi^{\alpha\mu\nu}(q, r, p)$ may be obtained by supplementing the $v_i^{\alpha\mu\nu}$ of Eq. (4.2) with 4 totally transverse tensors, say $\bar{t}_i^{\alpha\mu\nu}$, such that $q_\alpha \bar{t}_i^{\alpha\mu\nu} = r_\mu \bar{t}_i^{\alpha\mu\nu} = p_\nu \bar{t}_i^{\alpha\mu\nu} = 0$. For example, one could use the $\bar{t}_i^{\alpha\mu\nu}$ given in Eq. (3.6) of [90], corresponding to the transverse part of the Ball–Chiu (BC) basis [73]. However, the resulting basis, $v_i^{\alpha\mu\nu} \cup \bar{t}_j^{\alpha\mu\nu}$, introduces spurious divergences in certain form factors of the pole-free part, thus being unsuitable for many applications. Furthermore, as explained in [90], the BC basis is inconvenient for the description of $V^{\alpha\mu\nu}(q, r, p)$, because the 10 non-transverse tensors (the $\ell_i^{\alpha\mu\nu}$ in Eq. (3.4) of [90]) are not longitudinal⁵, in the sense that $P_{\alpha'\alpha}(q)P_{\mu'\mu}(r)P_{\nu'\nu}(p)\ell_i^{\alpha\mu\nu} \neq 0$. As a result, in the BC basis, the transverse components of $V^{\alpha\mu\nu}(q, r, p)$ acquire poles as well, which combine in complicated ways with the non-transverse ones to yield a strictly longitudinally coupled $V^{\alpha\mu\nu}(q, r, p)$. The basis of [91] appears to suffer from the same shortcoming. Thus, it is preferable to decompose the

⁵ In [73], the $\ell_i^{\alpha\mu\nu}$ span the part of the vertex that saturates the STI, which was denominated “longitudinal”, in contradistinction to the “transverse” (automatically conserved) component. The confusion caused by the fact that the $\ell_i^{\alpha\mu\nu}$ are not longitudinal, in the sense explained above, may be avoided by using the term “non-transverse” instead.

pole-free and pole parts in different bases, such as the BC for $\Gamma^{\alpha\mu\nu}(q, r, p)$ and Eq. (4.2) for $V^{\alpha\mu\nu}(q, r, p)$.

5 Mixed poles from the Slavnov–Taylor identity

In this section, we turn our attention to the STI satisfied by the full vertex $\Pi_{\alpha\mu\nu}(q, r, p)$. As we will show in detail, when the gluon propagator is finite at the origin (massive), the STI imposes an extended pole content on the three-gluon vertex. Specifically, the only way to achieve self-consistency is by introducing mixed poles in $V_{\alpha\mu\nu}(q, r, p)$; the form factors associated with these poles must satisfy strict constraints, which preclude their vanishing.

We emphasize that the central assumption underlying this analysis is that both the BRST symmetry⁶ and the associated STIs remain intact when the gluon acquires a mass through the action of the Schwinger mechanism. This assumption is strongly corroborated by the STI-driven extraction of the $\mathbb{C}(q)$ using lattice inputs [14, 63–65]; for a variety of related discussions and approaches, see [27, 36, 94–98], and references therein.

5.1 Abelian STI with a hard mass

To fix the ideas, let us consider first the simplified situation where the three-gluon vertex satisfies the Abelian STI given by

$$q^\alpha \Pi_{\alpha\mu\nu}(q, r, p) = P_{\mu\nu}(p)\Delta^{-1}(p) - P_{\mu\nu}(r)\Delta^{-1}(r). \tag{5.1}$$

Moreover, let the gluon propagator be given by the tree-level form, i.e., $\Delta^{-1}(q) \rightarrow q^2 - m^2$, corresponding to a simple massive propagator in Minkowski space.

Then, after substitution, the STI becomes

$$\begin{aligned} q^\alpha \Pi_{\alpha\mu\nu}(q, r, p) &= g_{\mu\nu}(p^2 - r^2) + r_\mu r_\nu - p_\mu p_\nu \\ &\quad + m^2 \left(\frac{p_\mu p_\nu}{p^2} - \frac{r_\mu r_\nu}{r^2} \right). \end{aligned} \tag{5.2}$$

Evidently, the form factors associated with the tensor structures $p_\mu p_\nu$ and $-r_\mu r_\nu$ on the r.h.s. of Eq. (5.2) contain poles in p^2 and r^2 , respectively, whose residue is m^2 . In fact, these tensor structures are longitudinal to the uncontracted legs of the vertex, i.e., those carrying momenta r and p .

Hence, the self-consistency of Eq. (5.2) requires that $\Pi_{\alpha\mu\nu}(q, r, p)$ should contain longitudinally coupled poles of the form r_μ/r^2 and p_ν/p^2 . Evidently, from the cyclic permutations of Eq. (5.2) (equivalently, from Bose symmetry),

⁶ We employ the *standard* BRST symmetry of QCD, to be distinguished from the modified BRST symmetry of the refined Gribov–Zwanziger action [92, 93].

$\Gamma_{\alpha\mu\nu}(q, r, p)$ must also contain massless poles longitudinally coupled to q_α , i.e., of the form q_α/q^2 . Thus, the STI implies that $\Gamma_{\alpha\mu\nu}(q, r, p)$ must assume the special form of Eq. (2.5), with a nonzero pole part, $V_{\alpha\mu\nu}(q, r, p)$.

At this point, let us assume that the pole-free part of the vertex, $\Gamma_{\alpha\mu\nu}(q, r, p)$, reduces to the tree-level form given in Eq. (3.4), i.e., $\Gamma_{\alpha\mu\nu}(q, r, p) \rightarrow \Gamma_{\alpha\mu\nu}^{(0)}(q, r, p)$, such that, from Eq. (2.5), $\Gamma_{\alpha\mu\nu}(q, r, p) = \Gamma_{\alpha\mu\nu}^{(0)}(q, r, p) + V_{\alpha\mu\nu}(q, r, p)$. Then, Eq. (5.2) can be recast into an STI for $V_{\alpha\mu\nu}(q, r, p)$, namely

$$q^\alpha V_{\alpha\mu\nu}(q, r, p) = m^2 \left(\frac{p_\mu p_\nu}{p^2} - \frac{r_\mu r_\nu}{r^2} \right), \tag{5.3}$$

together with its cyclic permutations.

Next, assume that $V_{\alpha\mu\nu}(q, r, p)$ satisfies the longitudinality condition of Eq. (3.1), as required by both the Schwinger mechanism and lattice QCD. Expanding out the transverse projectors in that equation, and using Eq. (5.3) and its permutations, one straightforwardly obtains

$$V_{\alpha\mu\nu}(q, r, p) = \frac{m^2}{2} \left[\frac{q_\alpha r_\mu}{q^2 r^2} (q - r)_\nu + \frac{r_\mu p_\nu}{r^2 p^2} (r - p)_\alpha + \frac{p_\nu q_\alpha}{p^2 q^2} (p - q)_\mu \right], \tag{5.4}$$

which shows that $V_{\alpha\mu\nu}(q, r, p)$ must contain mixed double poles, with residues proportional to the gluon mass. Note that this result amounts to the constant mass limit of the *Ansatz* given in [24], constructed therein for a momentum-dependent mass, $m^2(q)$. Furthermore, the combination $\Gamma_{\alpha\mu\nu}^{(0)}(q, r, p) + V_{\alpha\mu\nu}(q, r, p)$, with $V_{\alpha\mu\nu}(q, r, p)$ given by Eq. (5.4) reproduces the effective three-gluon vertex of Cornwall [99, 100]. Lastly, comparing Eqs. (4.4) and (5.4) we read off the expressions for the form factors

$$V_7(q, r, p) = V_8(q, r, p) = V_9(q, r, p) = \frac{m^2}{2}, \tag{5.5}$$

with all other V_i vanishing in this simple case.

If the form of the pole-free part is not known, as is generally the case, the complete momentum dependence of $V_{\alpha\mu\nu}(q, r, p)$ cannot be determined. Nevertheless, the values of the form factors $V_i(q, r, p)$ of Eq. (4.4) at zero momenta can be obtained unequivocally from the STI. In particular, in the toy model of Eq. (5.2)

$$V_9(q) = m^2/2, \tag{5.6}$$

independently of the exact form of $\Gamma_{\alpha\mu\nu}$, where we use Eq. (4.6) and define

$$V_9(q) := V_9(q, -q, 0) = V_9(0, q, -q). \tag{5.7}$$

Evidently, the same result holds for $V_8(q, -q, 0) = V_8(q, -q, 0) = V_7(q, 0, -q) = V_7(0, q, -q)$.

5.2 General case: mixed poles and the residue function

Having fixed the general ideas, we now turn to the full form of the STI, and demonstrate how to obtain from it expressions for the V_i when one of the momenta vanishes.

The STI is given by [72]

$$q^\alpha \Gamma_{\alpha\mu\nu}(q, r, p) = F(q) \left[\Delta^{-1}(p) P_\nu^\alpha(p) H_{\alpha\mu}(p, q, r) - \Delta^{-1}(r) P_\mu^\alpha(r) H_{\alpha\nu}(r, q, p) \right]; \tag{5.8}$$

the cases $r^\mu \Gamma_{\alpha\mu\nu}(q, r, p)$ and $p^\nu \Gamma_{\alpha\mu\nu}(q, r, p)$ are obtained from Eq. (5.8) through permutations of the appropriate momenta and indices. In the above equation, $F(q)$ is the ghost dressing function, defined in terms of the ghost propagator $D^{ab}(q) = i\delta^{ab}D(q)$ by $D(q) = F(q)/q^2$, while $H_{\mu\nu}(r, q, p)$ represents the ghost–gluon scattering kernel, with r, q, p denoting the momenta of the anti-ghost, ghost, and gluon, respectively.

The most general Lorentz structure of $H_{\mu\nu}(r, q, p)$ is given by [101]

$$H_{\mu\nu}(r, q, p) = g_{\nu\mu} A_1 + r_\mu r_\nu A_2 + p_\mu p_\nu \mathbb{A}_3 + p_\mu r_\nu A_4 + r_\mu p_\nu \mathbb{A}_5, \tag{5.9}$$

where $A_i \equiv A_i(r, q, p)$ and $\mathbb{A}_i \equiv \mathbb{A}_i(r, q, p)$; the use of distinct notation for the third and fifth form factors will become clear in what follows. At tree level, $A_1^{(0)} = 1$, while all other form factors vanish. Note that since in Eq. (5.8) the $H_{\mu\nu}(r, q, p)$ is contracted by transverse projectors, only the form factors A_1, A_4 and \mathbb{A}_3 contribute to the STI.

At this point, it is crucial to recognize that the Schwinger mechanism induces poles not only to the vertex $\Gamma_{\alpha\mu\nu}(q, r, p)$ but also to the ghost–gluon kernel $H_{\mu\nu}(r, q, p)$. In particular, the poles are longitudinally coupled, carrying the momentum and Lorentz index of the incoming gluon leg. Therefore, they are contained in the form factors $\mathbb{A}_{3,5}(r, q, p)$, which assume the general form

$$\mathbb{A}_{3,5}(r, q, p) = \frac{A_{3,5}^{\mathbf{P}}(r, q, p)}{p^2} + A_{3,5}(r, q, p), \tag{5.10}$$

where $A_{3,5}(r, q, p)$ denotes the pole-free part.

To determine the residues of the poles required by the STI, we begin by decomposing both sides of Eq. (5.8) in the same basis and equating coefficients of independent tensor structures. Since the tensors appearing in the STI have two free Lorentz indices and two independent momenta, they can all be decomposed in the same basis employed for $H_{\mu\nu}(r, q, p)$ in Eq. (5.9). In particular, the contracted pole-free part may

be written as

$$q^\alpha \Gamma_{\alpha\mu\nu}(q, r, p) = S_1 g_{\mu\nu} + S_2 r_\mu r_\nu + S_3 p_\mu p_\nu + S_4 p_\mu r_\nu + S_5 r_\mu p_\nu, \tag{5.11}$$

with $S_i \equiv S_i(q, r, p)$. At tree level, $S_1^{(0)} = p^2 - r^2$, $S_2^{(0)} = 1$, $S_3^{(0)} = -1$, and $S_4^{(0)} = S_5^{(0)} = 0$. Note that, from Bose symmetry, S_1 , S_4 and S_5 must be anti-symmetric under the exchange of $r \leftrightarrow p$, such that

$$S_1(0, r, -r) = S_4(0, r, -r) = S_5(0, r, -r) = 0. \tag{5.12}$$

Then, since $\Gamma_{\alpha\mu\nu}(q, r, p)$ is pole-free, its contraction with q^α vanishes when $q = 0$, such that Eqs. (5.11) and (5.12) imply also that

$$S_2(0, r, -r) = -S_3(0, r, -r). \tag{5.13}$$

As for the pole part, after contracting Eq. (4.4) with q^α , we obtain

$$q^\alpha V_{\alpha\mu\nu}(q, r, p) = V_1 g_{\mu\nu} + \frac{\bar{V}_2}{r^2} r_\mu r_\nu + \frac{\bar{V}_3}{p^2} p_\mu p_\nu + V_2 p_\mu r_\nu + \frac{\bar{V}_5}{r^2 p^2} r_\mu p_\nu, \tag{5.14}$$

with the $\bar{V}_i \equiv \bar{V}_i(q, r, p)$ given by

$$\begin{aligned} \bar{V}_2 &= -V_3 - (p \cdot q)V_4 - 2V_7, \\ \bar{V}_3 &= -V_5 - (r \cdot q)V_6 + 2V_9, \\ \bar{V}_5 &= V_{10} + (p^2 - r^2)V_8 - p^2 [V_3 + (q \cdot p)V_4 + V_7] \\ &\quad - r^2 [V_5 + (q \cdot r)V_6 - V_9]. \end{aligned} \tag{5.15}$$

As in the previous subsection, we now isolate the tensor structures $r_\mu r_\nu$ and $p_\mu p_\nu$ on both sides of Eq. (5.8); equating their coefficients yields

$$\begin{aligned} S_2 &= \frac{1}{r^2} \left\{ F(q) \left[\Delta^{-1}(r) [A_1(r, q, p) + (p \cdot r)A_4(r, q, p)] \right. \right. \\ &\quad \left. \left. + r^2 \Delta^{-1}(p) \mathbb{A}_3(p, q, r) \right] - \bar{V}_2 \right\}, \\ S_3 &= -\frac{1}{p^2} \left\{ F(q) \left[p^2 \Delta^{-1}(r) \mathbb{A}_3(r, q, p) + \Delta^{-1}(p) \right. \right. \\ &\quad \left. \left. \times [A_1(p, q, r) + (p \cdot r)A_4(p, q, r)] \right] + \bar{V}_3 \right\}. \end{aligned} \tag{5.16}$$

Since S_3 is pole-free by definition, in the limit $p \rightarrow 0$, the term $1/p^2$ must be canceled by the content of the curly bracket in Eq. (5.16). Thus, what appears to be a pole in p^2 must be converted into an evitable singularity. The condition for this to occur is given by

$$V_9(q) = \frac{F(q)}{2} \left[m^2 A_1(q) - \Delta^{-1}(q) A_3^{\mathbf{P}}(q) \right], \tag{5.17}$$

where $m^2 = -\Delta^{-1}(0)$, in Minkowski space, and we used Eq. (5.10) and defined

$$A_1(q) := A_1(0, q, -q), \quad A_3^{\mathbf{P}}(q) := A_3^{\mathbf{P}}(q, -q, 0). \tag{5.18}$$

Note that setting the ghost-sector Green's functions in Eq. (5.17) to their tree level expressions in Eq. (5.17), i.e., $F \rightarrow 1$, $A_1 \rightarrow 1$ and $\mathbb{A}_3 \rightarrow 0$, leads to Eq. (5.6).

Similarly, the requirement that the S_2 of Eq. (5.16) be pole-free at $r = 0$ yields a relation identical to Eq. (5.17), but with $V_9(q)$ substituted by $V_7(0, q, -q)$. This last result follows also from Bose symmetry, according to Eq. (4.6). For the same reason, Eq. (5.17) also holds with the left-hand side substituted by any one of $V_7(0, q, -q)$, $V_8(q, -q, 0)$, and $V_8(q, 0, -q)$.

Returning to Eq. (5.17), it is clear that the only way for V_9 to vanish identically for all q (i.e., for $V_{\alpha\mu\nu}$ not to contain the associated mixed pole) is for the r.h.s. to also vanish; however, at least when $q = 0$, this cannot happen in the Landau gauge. Indeed, as was demonstrated in [102], in this gauge,

$$A_1(0) = \tilde{Z}_1, \quad A_3^{\mathbf{P}}(0) = 0, \tag{5.19}$$

where \tilde{Z}_1 is the renormalization constant of the ghost-gluon vertex, which is *finite* by virtue of Taylor's theorem [70]. Hence, at the origin, Eq. (5.17) reduces to

$$V_9(0) = \frac{1}{2} \tilde{Z}_1 F(0) m^2. \tag{5.20}$$

Consequently, just as in the toy model of Eq. (5.2), the self-consistency of the full STI in the presence of an infrared finite gluon propagator requires the appearance of a pole associated with the form factor V_9 .

The function $V_9(q)$, associated with the mixed pole $1/q^2 p^2$ will be particularly important in the analysis that follows. To understand its nature, consider a function of two variables, x and y of the form $f(x, y) = g(x, y)/xy$, with $g(x, 0) \neq 0$ and $g(0, y) \neq 0$, such that $f(x, y)$ has simple poles as $x \rightarrow 0$ and $y \rightarrow 0$. In particular, if we take $y \rightarrow 0$, the residue of this pole is a function of x , given by $r(x) = g(x, 0)/x$. In fact, if we subsequently take $x \rightarrow 0$, $g(0, 0) \neq 0$ is the residue of the function $r(x)$. Evidently, in this analogy, $g(x, 0)$ plays the role of $V_9(q)$; in what follows, we will refer to $V_9(q)$ as the “*residue function*”.

We conclude this discussion by pointing out that the tensor structures $g_{\mu\nu}$, $r_\nu p_\mu$ and $r_\mu p_\nu$ of Eq. (5.8), associated with the pole-free form factors $S_{1,4,5}$, lead to constraints on the behavior of the remaining form factors, V_i , which are absent from the simplified result of Eq. (5.4). These additional relations, however, constrain certain derivatives of the V_i , rather than the values of the form factors themselves. Indeed, the

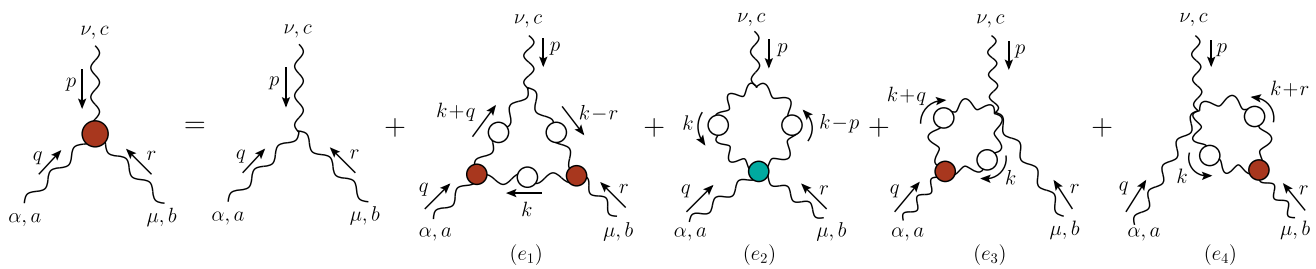


Fig. 7 The diagrams contributing to the truncated SDE for three-gluon vertex that we employ; ghost and two-loop diagrams have been omitted. The swordfish diagrams ($e_{2,3,4}$) carry a symmetry factor of $1/2$

constraint obtained from $g_{\mu\nu}$ is equivalent to the so-called “Ward Identity displacement”, which has been analyzed in detail in recent works [13, 14, 63, 64]. On the other hand, the $r_\mu p_\nu$ structure leads to a constraint on the form factor V_{10} , which amounts to a drastic reduction of the triple pole associated with it; the detailed demonstration of this point is given in Sect. 8.

6 Residue function from the Schwinger–Dyson equation

The special relation given in Eq. (5.17) implies that, in the presence of an infrared finite gluon propagator, the appearance of mixed poles in the three-gluon vertex is an inevitable requirement of the STI. In this section we explore this same relation from the point of view of the SDE satisfied by the three-gluon vertex. Specifically, we will show that, when the dynamical structures imposed by the activation of the Schwinger mechanism are duly taken into account, a truncated form of the vertex SDE leads to an approximate version of Eq. (5.17).

6.1 General considerations

In order to obtain from the vertex SDE the relation satisfied by the residue function $V_9(q)$ in Eq. (5.17), we follow the same procedure employed in its derivation from the STI: (i) we begin by contracting the vertex SDE by q_α ; (ii) then, we isolate the tensor structure $p_\mu p_\nu$ from the result, which yields $\bar{V}_3/p^2 + S_3$ [recall Eqs. (5.11) and (5.14)]; (iii) finally, we multiply by p^2 and take the limit $p = 0$, where $\bar{V}_3(q, r, p) \rightarrow 2V_9(q)$ [see Eq. (5.15)].

To streamline the application of this procedure, it is convenient to set up the vertex SDE with tree-level vertices in the leg carrying momentum p , as in Fig. 7, rather than the version shown in Fig. 1. With this choice, the contraction of the SDE by q^α triggers inside the diagrams the STIs for the fully dressed vertices, with an incoming q -leg. These STIs, in turn, simplify the identification of certain pole contributions stemming from the four-gluon vertex, as we will see shortly.

We emphasize that the SDE given in Fig. 7 is truncated, by keeping only “one-loop dressed diagrams” containing gluons and the massless composite excitations associated with the Schwinger mechanism. Note, in particular, the absence of contributions originating from the ghost loop denoted by (c_2) in Fig. 3, and that the only representatives from graph (c_3) are diagrams (e_3) and (e_4). Given this truncation, we do not expect to reproduce Eq. (5.17) in its entirety; in particular, it is reasonable to expect that the term m^2 will be approximated by its one-loop dressed gluonic expression, $m_{(a_1)}^2$, given in Eq. (2.9). As we will see in what follows, this is indeed what happens.

Recalling the diagrammatic analysis presented in Sect. 3, it is relatively straightforward to establish that diagrams (e_1), (e_3), and (e_4) contain poles in the q - and r -channels, but not in the p -channel, which is relevant for the derivation of Eq. (5.17).

Instead, (e_2) possesses a pole in the p -channel, as may be deduced by means of two different (but ultimately equivalent) arguments, both related to the nature of the fully-dressed four-gluon vertex [103–113], $\Pi_{\alpha\mu\delta\tau}^{abts}$.

The first argument is based on the observation that the special diagram (d_2) of Fig. 3 is part of $\Pi_{\alpha\mu\delta\tau}^{abts}$; evidently, since the vertex SDE is now written with respect to the p -leg, the appropriate replacement (e.g., $q \rightarrow p$) must be carried out in (d_2), which acquires thusly a massless bound state propagator i/p^2 .

The second is by noticing that the STI satisfied by $\Pi_{\alpha\mu\delta\tau}^{abts}$ generates naturally a pole in the p -channel, provided that the poles of the three-gluon vertices appearing in its r.h.s. are properly included. Specifically, the STI reads [39, 114, 115]

$$\begin{aligned}
 q^\alpha \Pi_{\alpha\mu\delta\tau}^{abts}(q, r, p - k, k) &= F(q) [f^{tad} f^{dbs} H^\gamma_\delta \\
 &\times (k + r, q, p - k) \Pi_{\gamma\mu\tau}(-k - r, r, k) \\
 &+ f^{sad} f^{dbt} H^\gamma_\tau(-k - q, q, k) \Pi_{\gamma\mu\delta}(k + q, r, p - k) \\
 &+ f^{bad} f^{dst} H^\gamma_\mu(p, q, r) \underbrace{\Pi_{\gamma\tau\delta}(-p, k, p - k)}_{\text{Contains } \frac{p^\gamma}{p^2}}] + \dots,
 \end{aligned}
 \tag{6.1}$$

where the ellipsis denotes terms involving a ghost–ghost–gluon–gluon scattering kernel. Since this kernel has no tree-level value [39, 115], we expect it to be subleading and omit it from our treatment. Evidently, the full three-gluon vertices appearing on the r.h.s. of Eq. (6.1) enter with their entire pole content. In particular, the underbrace in that equation highlights the explicit appearance of a p_γ/p^2 term, originating from the vertex $\Pi_{\gamma\tau\delta}(-p, k, p - k)$.

It is clear that the two arguments presented above are interlinked: the r.h.s. of the STI in Eq. (6.1) contains a pole in $1/p^2$ because diagram (d_2) is part of the four-gluon vertex, whose contraction by q^α appears on the l.h.s. This accurate balance evidences once again the harmonious interplay between symmetry and dynamics.

6.2 The derivation

Armed with these observations, we now proceed to the derivation of Eq. (5.17), following the three main steps, (i)–(iii), mentioned above.

To that end, we start from the complete expression for (e_2),

$$(e_2)_{\alpha\mu\nu}^{abc} = -\frac{ig^2 Z_3}{2} \int_k \Delta^{\rho\delta}(k-p) \Delta^{\sigma\tau}(k) \Gamma_{\nu\sigma\rho}^{(0)} \times (-p, k, p-k) f^{cst} \Pi_{\alpha\mu\delta\tau}^{abts}(q, r, p-k, k), \tag{6.2}$$

where we have factored out a g .

Then, following step (i), we contract Eq. (6.2) with q^α , thus triggering the STI of Eq. (6.1). Then, Eq. (6.2) yields

$$q^\alpha (e_2)_{\alpha\mu\nu} = -\frac{\lambda Z_3 F(q)}{p^2} \int_k \Delta^{\rho\delta}(k-p) \Delta^{\sigma\tau}(k) \Gamma_{\nu\sigma\rho}^{(0)} \times (-p, k, p-k) p^\gamma H_{\gamma\mu}(p, q, r) \times [V_1(-p, k, p-k) g_{\delta\tau} + V_2(-p, k, p-k) p_\delta p_\tau] + \dots, \tag{6.3}$$

where the color structure f^{abc} has been canceled out from both sides, and the ellipsis denotes terms that do not contain $1/p^2$ poles, and thus cannot contribute to $V_9(q)$.

Next, we evaluate the term $p^\gamma H_{\gamma\mu}(p, q, r)$ appearing in Eq. (6.3) using the well-known STI [72]

$$p^\gamma H_{\gamma\mu}(p, q, r) = \Pi_\mu(p, q, r), \tag{6.4}$$

where $\Pi_\mu^{abc}(p, q, r) = -g f^{abc} \Gamma_\mu(p, q, r)$ is the ghost–gluon vertex, whose most general Lorentz decomposition reads [67, 101, 116]

$$\Pi_\mu(p, q, r) = p_\mu B_1(p, q, r) + r_\mu \mathbb{B}_2(p, q, r). \tag{6.5}$$

Then, it follows from Eq. (6.4) that

$$p^\gamma H_{\gamma\mu}(p, q, r) = p_\mu B_1(p, q, r) + r_\mu \mathbb{B}_2(p, q, r), \tag{6.6}$$

while Eq. (5.9) allows us to write the B_i in terms of the A_i and \mathbb{A}_i as [101, 116]

$$B_1(p, q, r) = A_1(p, q, r) + p^2 A_2(p, q, r) + (p \cdot r) A_4(p, q, r), \tag{6.7}$$

$$\mathbb{B}_2(p, q, r) = (p \cdot r) \mathbb{A}_3(p, q, r) + p^2 \mathbb{A}_5(p, q, r).$$

Note that, since $\mathbb{A}_i(p, q, r)$ displays a pole when $r = 0$, so does the $\mathbb{B}_2(p, q, r)$; the pole amplitude associated with the ghost–gluon vertex has been studied in detail in [33, 43, 63].

Now, we proceed to step (ii). Clearly, only the term $p_\mu B_1(p, q, r)$ of Eq. (6.6) can contribute to the tensor structure $p_\mu p_\nu$, once inserted in Eq. (6.3) for $q^\alpha (e_2)_{\alpha\mu\nu}$. Hence, we can write

$$q^\alpha (e_2)_{\alpha\mu\nu} = -\frac{\lambda Z_3 F(q) B_1(p, q, r) p_\mu}{p^2} \int_k \Delta^{\rho\delta}(k-p) \Delta^{\sigma\tau}(k) \times \Gamma_{\nu\sigma\rho}^{(0)}(-p, k, p-k) \times [V_1(-p, k, p-k) g_{\delta\tau} + V_2(-p, k, p-k) p_\delta p_\tau] + \dots, \tag{6.8}$$

where the ellipsis now denotes terms that cannot contribute to $V_9(q)$ because they do not contain either a $1/p^2$ or a p_μ .

In anticipation of the fact that we will take $p \rightarrow 0$ at the end of the calculation, we can already consider p to be small. In this case, we can use into Eq. (6.8) the Taylor expansion given in Eq. (2.8), and its analog with V_1 substituted by V_2 . Then, one sees that the term $V_2(-p, k, p-k)$ cannot contribute to $V_9(q)$, since it is two orders higher in p than $V_1(-p, k, p-k)$. Hence, we obtain explicitly

$$q^\alpha (e_2)_{\alpha\mu\nu} = 3\lambda Z_3 F(q) B_1(p, q, r) \left(\frac{p_\mu p_\nu}{p^2} \right) \times \int_k k^2 \Delta^2(k) \mathbb{C}(k) + \dots, \tag{6.9}$$

with the ellipsis now including terms that are higher-order in the Taylor expansion around $p = 0$.

At this point, recalling Eqs. (5.14) and (5.15), the scalar coefficient of $p_\mu p_\nu$ in Eq. (6.9) yields a contribution to $\overline{V}_3/p^2 + S_3$, namely

$$\overline{V}_3^{(e_2)}(p, q, r)/p^2 + S_3^{(e_2)}(p, q, r) = \frac{1}{p^2} F(q) B_1(p, q, r) \times \left[3\lambda Z_3 \int_k k^2 \Delta^2(k) \mathbb{C}(k) \right] + \dots, \tag{6.10}$$

where the superscript “ (e_2) ” emphasizes that the above expression contains only the contribution from diagram (e_2).

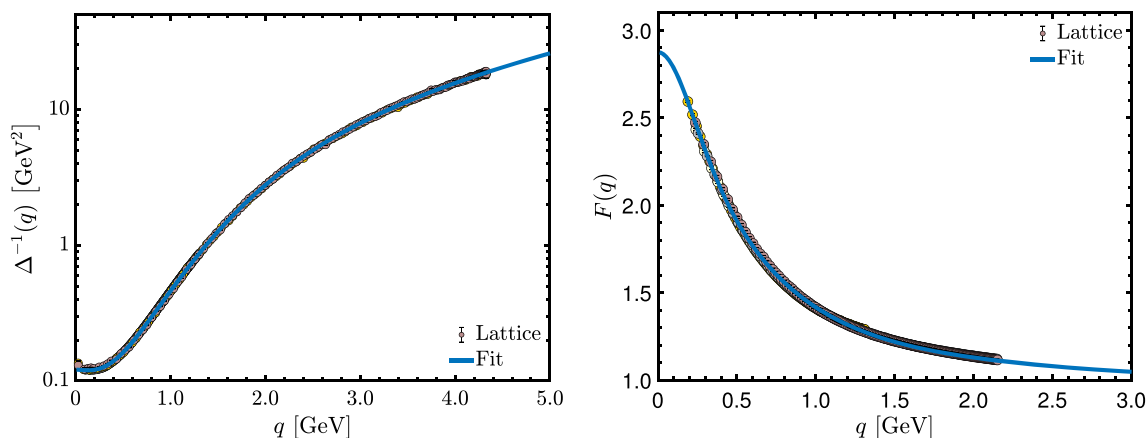


Fig. 8 Lattice data (points) of [67] for $\Delta^{-1}(q)$ (left) and $F(q)$ (right), together with their corresponding fits (blue solid lines), given by Eqs. (C6) and (C11) of [63], respectively

Lastly, we perform step (iii), i.e., multiply Eq. (6.10) by p^2 and set $p = 0$. In doing so, we note from Eq. (6.7) that $B_1(0, q, -q) = A_1(q)$, while Eqs. (4.8) and (5.15) imply that $\bar{V}_3^{(e_2)}(0, q, -q) = 2V_9^{(e_2)}(q)$. Furthermore, since (e_2) is the only diagram of Fig. 7 that contributes to $V_9(q)$, we have $V_9(q) = V_9^{(e_2)}(q)$, such that

$$\begin{aligned}
 V_9(q) &= F(q)A_1(q) \left[\frac{3\lambda Z_3}{2} \int_k k^2 \Delta^2(k) \mathbb{C}(k) \right] \\
 &= \frac{1}{2} F(q)A_1(q)m_{(a_1)}^2, \tag{6.11}
 \end{aligned}$$

where we used Eq. (2.9) to obtain the last equality.

Therefore, the SDE of Fig. 7 satisfies an approximate form of Eq. (5.17), where only the term containing $A_3^p(q)$ in that equation is absent. This term could arise in the full SDE either from the diagrams that we omitted in Fig. 7, or from the ghost–ghost–gluon–gluon kernel that we dropped in Eq. (6.1); its proper restoration requires a detailed treatment that goes beyond the scope of the present work.

Finally, we point out that, at $q = 0$, the SDE result for $V_9(0)$ satisfies the STI requirement of Eq. (5.20) exactly, by virtue of Eq. (5.19).

7 Computing the residue function

We next turn to the numerical determination of the residue function, $V_9(q)$, from Eq. (5.17). To this end, we first transform Eq. (5.17) to Euclidean space, to obtain

$$V_9(q) = \frac{F(q)}{2} \left[m^2 A_1(q) + \Delta^{-1}(q) A_3^p(q) \right]. \tag{7.1}$$

As we will explain below, for the determination of $A_3^p(q)$ we will make use of the displacement function $\mathbb{C}(q)$, shown in Fig. 2. Since in [64,65] the $\mathbb{C}(q)$ has been computed in

the so-called “asymmetric MOM scheme” [52,54,67,102], with $\mu = 4.3$ GeV, the same renormalization prescription will be employed in what follows. Note that, in this scheme, the finite ghost–gluon renormalization constant appearing in Eqs. (5.19) and (5.20) is given by $\tilde{Z}_1 = 0.9333$ [14,64].

Then, for the $F(q)$ and $\Delta(q)$ appearing in Eq. (7.1) we use physically motivated fits to lattice data of [67], given by Eqs. (C6) and (C11) of [63], respectively. These fits are shown as continuous blue lines in Fig. 8, where they are compared to the lattice data of [67] (points). Note that the value of $\Delta^{-1}(0) = 0.121$ GeV $^{-2}$ corresponding to this fit leads to the previously mentioned value of $m = 348$ MeV for $\mu = 4.3$ GeV. Moreover, the fitting functions for both $\Delta(q)$ and $F(q)$ were constructed in such a way that they reproduce the respective one-loop resummed anomalous dimensions.

For the tree-level (classical) form factor $A_1(q)$ of the ghost–gluon kernel, we employ the result of the SDE analysis of [101]⁷; the result is shown as red squares in the left panel of Fig. 9, and is seen to deviate by at most 11%, at $q = 1.43$ GeV, from the tree-level value, $A_1^{(0)}(q) = 1$.

Then, the only unknown ingredient in Eq. (7.1) is the ghost–gluon pole term $A_3^p(q)$, which may be computed as follows. We start with the one-loop dressed truncation of the SDE describing the ghost–gluon kernel, $H_{\mu\nu}(r, q, p)$, see, e.g., Fig. 3 of [101]. From this SDE, we derive a dynamical equation for $\mathbb{A}_3(r, q, p)$, using the projector $\mathcal{T}_3^{\mu\nu}$, given in Eqs. (3.7) and (3.8) of [101]. Then, recalling Eq. (5.10), we obtain $A_3^p(q)$ from the equation for $\mathbb{A}_3(r, q, p)$ by multiplying it by p^2 and taking the limit $p \rightarrow 0$. This procedure furnishes a linear integral equation for $A_3^p(q)$, which has the

⁷ In [101] the Taylor scheme [117–120] was employed; the conversion to the asymmetric scheme proceeds through the relation $A_1^{\text{asym}} = \tilde{Z} A_1^{\text{Taylor}}$.

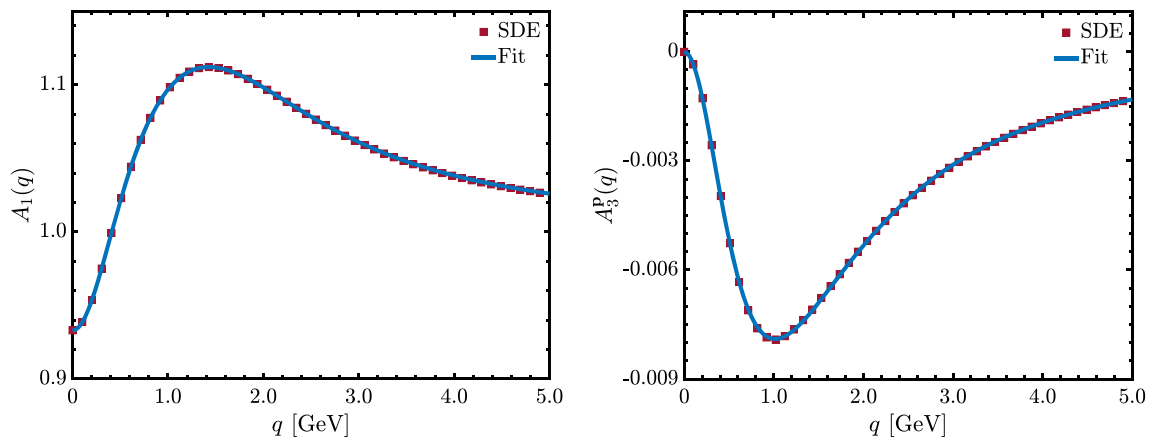


Fig. 9 Left: the form factor $A_1(q)$ of the ghost–gluon kernel, in the soft-antighost limit, taken from [101]. Right: pole amplitude $A_3^P(q)$ of the ghost–gluon kernel, computed from the truncated SDE of Eq. (7.2)

form

$$A_3^P(q) = \int_k \mathcal{K}_1(k, q) A_3^P(k) + \int_k \mathcal{K}_2(k, q) \mathbb{C}(k), \quad (7.2)$$

where we notice the appearance of $\mathbb{C}(q)$, and the kernels $\mathcal{K}_i(k, q)$ are comprised by combinations of Δ , F , and kinematic factors.

Then, we solve Eq. (7.2) numerically through the Nystrom method [121], employing for $\mathbb{C}(q)$ the result of [64, 65], shown in Fig. 2. Through this procedure, we obtain the result shown as red squares in the right panel of Fig. 9.

For convenience, we provide fits for the functions $A_1(q)$ and $A_3^P(q)$, which, in conjunction with the fits for $\Delta(q)$ and $F(q)$, allow $V_9(q)$ to be computed most expeditiously. Specifically, both $A_1(q)$ and $A_3^P(q)$ can be accurately fitted by the low-degree rational functions

$$A_1(q) = \tilde{Z}_1 [1 + R_1(q)], \quad A_3^P(q) = \tilde{Z}_1 R_2(q), \quad (7.3)$$

where

$$R_1(q) = \frac{q^2/a_1 + (q^2/a_2)^2 + (q^2/a_3)^3}{1 + q^2/b_1 + (q^2/b_2)^2 + (q^2/b_3)^3},$$

$$R_2(q) = \frac{q^2/c_1}{1 + q^2/d_1 + (q^2/d_2)^2}, \quad (7.4)$$

with fitting parameters given by $a_1 = 1.71 \text{ GeV}^2$, $a_2 = 2.68 \text{ GeV}^2$, $a_3 = 4.51 \text{ GeV}^2$, $b_1 = 0.410 \text{ GeV}^2$, $b_2 = 1.30 \text{ GeV}^2$, $b_3 = 1.89 \text{ GeV}^2$, $c_1 = -27.3 \text{ GeV}^2$, $d_1 = 0.419 \text{ GeV}^2$ and $d_2 = 1.03 \text{ GeV}^2$.

We emphasize that the fits in Eq. (7.3) preserve certain limits of the original functions, A_1 and A_3^P . First, at the origin, the fits for $A_1(q)$ and $A_3^P(q)$ satisfy Eq. (5.19). Next, a one-loop calculation reveals that, at large values of the momentum, $A_1(q)$ saturates to a constant [101]; in addition,

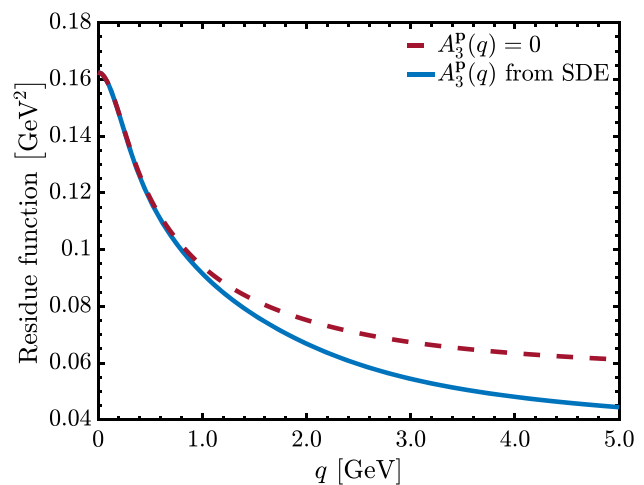


Fig. 10 Residue function, $V_9(q)$, computed from Eq. (5.17), using the $A_3^P(q)$ shown in Fig. 9 (blue continuous), compared to the result obtained if $A_3^P(q)$ is set to zero (red dashed line)

the numerical SDE result indicates that, in the same kinematic limit, $A_3^P \sim 1/q^2$. It is straightforward to verify that these ultraviolet features are correctly captured by the fits given by Eq. (7.3).

Using the above ingredients in Eq. (7.1), we obtain the $V_9(q)$ shown as a solid blue curve in Fig. 10. Comparing this result to that for $F(q)$, shown in the right panel of Fig. 8, it is clear that the shape of $V_9(q)$ is dominated by the ghost dressing function in Eq. (7.1).

Next, we test the effect of A_3^P on V_9 . To this end, we set $A_3^P(q)$ to zero in Eq. (7.1), in which case we obtain the result shown as a red dashed line in Fig. 10. Note that the latter becomes equal to the full result (blue continuous) at $q = 0$, by virtue of Eq. (5.19), but differs significantly from it for $q > 1 \text{ GeV}$.

To understand this difference, let us note that although $A_3^P(q)$ itself is small in comparison to the corresponding pole of the three-gluon vertex, $\mathbb{C}(q)$ [cf. Fig. 2 and Fig. 9], or even the saturation value of $V_9(q)$, it appears multiplied by $\Delta^{-1}(q)$. Since the latter increases rapidly in the ultraviolet, the product $A_3^P(q)\Delta^{-1}(q)$ can contribute a considerable amount to $V_9(q)$ at large q , as indeed is observed.

8 Absence of mixed triple pole

In this section, we analyze the infrared behavior of the form factor $V_{10}(q, r, p)$, which is accompanied by a denominator $q^2 r^2 p^2$ in Eq. (4.4). As such, at first sight, one expects that this term should act as a triple mixed pole.

Consider, for instance, taking all momenta to zero by first taking $p \rightarrow 0$, which implies also $r = -q$, and then taking $q \rightarrow 0$. In this case, if $V_{10}(0, 0, 0)$ were nonvanishing, one would have

$$\lim_{q,p \rightarrow 0} \frac{V_{10}(q, r, p)}{q^2 r^2 p^2} = \frac{V_{10}(0, 0, 0)}{q^4 p^2}, \tag{8.1}$$

where we use the shorthand notation

$$\lim_{q,p \rightarrow 0} := \lim_{q \rightarrow 0} \lim_{p \rightarrow 0}. \tag{8.2}$$

However, as we will demonstrate in Sect. 8.1, the STI of Eq. (5.8) requires $V_{10}(q, r, p)$ to vanish in this limit as

$$\lim_{q,p \rightarrow 0} V_{10}(q, r, p) = 2(q \cdot p)q^2 f(0), \tag{8.3}$$

where $f(q)$ is some pole-free function at $q = 0$. Consequently, in Euclidean space,

$$\lim_{q,p \rightarrow 0} \frac{V_{10}(q, r, p)}{q^2 r^2 p^2} = \lim_{q,p \rightarrow 0} \frac{2 \cos \theta}{|q||p|} f(0), \tag{8.4}$$

where $q \cdot p = |q||p| \cos \theta$ and $|q|$ denotes the magnitude of the Euclidean momentum q .

Moreover, an approximate SDE analysis presented in Sect. 8.2 shows that this particular requirement is enforced by the Schwinger mechanism, and especially due to the validity of Eq. (2.8).

Note that the divergence in Eq. (8.4) is in fact weaker than that associated with the form factors V_7, V_8 , and V_9 , namely

$$\lim_{q,p \rightarrow 0} \frac{V_9(q, r, p)}{q^2 p^2} = \lim_{q,p \rightarrow 0} \frac{\tilde{Z}_1 F(0)m^2}{2q^2 p^2}, \tag{8.5}$$

where we used Eq. (5.20).

8.1 Demonstration from the STI

For the derivation of Eq. (8.3) from the STI of Eq. (5.8), we begin by noting that Eq. (4.8) already implies that

$$\begin{aligned} \lim_{p \rightarrow 0} V_{10}(q, r, p) &= 2(p \cdot q)V'_{10}(q), \\ V'_{10}(q) &:= \left[\frac{\partial V_{10}(q, r, p)}{\partial r^2} \right]_{p=0}. \end{aligned} \tag{8.6}$$

Then, to obtain Eq. (8.3) we need to show that

$$\lim_{q \rightarrow 0} V'_{10}(q) = q^2 f(0). \tag{8.7}$$

In order to constrain V_{10} from the STI, let us first note that this form factor appears in Eq. (5.8) through the combination \bar{V}_5 , defined in Eqs. (5.14) and (5.15). Then, isolating its respective tensor structure, $r_\mu p_\nu$, and equating the corresponding coefficients on each side of Eq. (5.8), we obtain

$$\begin{aligned} S_5 &= \frac{1}{r^2 p^2} \left\{ (p \cdot r)F(q) \left[p^2 \Delta^{-1}(r) \mathbb{A}_3(r, q, p) \right. \right. \\ &\quad \left. \left. - r^2 \Delta^{-1}(p) \mathbb{A}_3(p, q, r) \right] - \bar{V}_5 \right\}, \end{aligned} \tag{8.8}$$

where we note the term $r^2 p^2$ in the denominator. Since S_5 is pole-free, the r.h.s of Eq. (8.8) must be an evitable singularity at $p = 0$ and $r = 0$, which implies that the term in curly brackets must vanish sufficiently fast in those limits.

Then, since S_5 is antisymmetric under the exchange of r and p , it suffices to consider the $p = 0$ limit of Eq. (8.8); hence, we expand the term in brackets around $p = 0$.

Using the Bose symmetry relations of Eqs. (4.6) and (4.7), it is straightforward to show that the zeroth order term vanishes. However, the linear term yields the nontrivial constraint

$$\begin{aligned} \bar{V}'_5(q) &= -\frac{F(q)}{2} \left\{ m^2 \left[q^2 A_3(0, q, -q) + A_3^P(0, q, -q) \right] \right. \\ &\quad \left. + \Delta^{-1}(q) A_3^P(q) \right\}, \end{aligned} \tag{8.9}$$

where we emphasize that $A_3^P(q)$ [see Eq. (5.18)] corresponds to a kinematic limit (soft-gluon) different from $A_3^P(0, q, -q)$ (soft-antighost), and define

$$\bar{V}'_5(q) := \left[\frac{\partial V_5(q, r, p)}{\partial r^2} \right]_{p=0}. \tag{8.10}$$

Next, we further expand Eq. (8.9) around $q = 0$. The zeroth order term is easily seen to vanish, while the first nonvanishing term is given by

$$\bar{V}'_5(q) = q^2 f_1(0), \tag{8.11}$$

where

$$f_1(0) := -\frac{F(q)m^2}{2} \left\{ A_3(0, 0, 0) + \left[\frac{d}{dq^2} (A_3^{\mathbf{P}}(0, q, -q) - A_3^{\mathbf{P}}(q, -q, 0)) \right]_{q=0} \right\}. \tag{8.12}$$

Then we relate V'_{10} to \bar{V}'_5 by expanding Eq. (5.15) around $p = 0$. In doing so, we make extensive use of the Bose symmetry relations of Eqs. (4.6) and (4.7), and invoke Eq. (2.8). After some algebra, this procedure yields

$$V'_{10}(q) = \bar{V}'_5(q) + q^2 f_2(q), \tag{8.13}$$

where

$$f_2(q) := \mathbb{C}(q) - q^2 \left[\frac{\partial V_2(p, q, r)}{\partial r^2} \right]_{p=0} + \left[\frac{\partial}{\partial r^2} (V_7(r, p, q) - V_7(q, p, r)) \right]_{p=0}. \tag{8.14}$$

Finally, combining Eqs. (8.11) and (8.13) we obtain the announced result, Eq. (8.7), by identifying $f(0) := f_1(0) + f_2(0)$.

8.2 SDE realization

Now, we show how Eq. (8.7) follows from the SDE of the three-gluon vertex. Note that, by virtue of Eq. (8.13), which is a consequence of Bose symmetry, it suffices to demonstrate Eq. (8.11).

To this end, we employ a procedure similar to that used in Sect. 6 to obtain $V_9(q)$. Specifically, (i) we contract the vertex SDE of Fig. 7 by q_α ; (ii) then, we isolate the tensor structure $r_\mu p_\nu$ from the result, which yields a contribution to $\bar{V}_5/(r^2 p^2) + S_5$; (iii) next, we multiply the result by $r^2 p^2$ and expand to lowest order in $p = 0$, thus obtaining \bar{V}'_5 ; (iv) lastly, we expand \bar{V}'_5 to lowest order around $q = 0$.

In carrying out step (i) above, we note that diagrams (e_1) , (e_3) and (e_4) of Fig. 7 do not contribute to V_{10} , for the exact same reasons that they do not contribute to V_9 , as discussed in Sect. 6. Hence, we focus on diagram (e_2) . Moreover, after triggering the STI of Eq. (6.1) for the four-gluon vertex in (e_2) , we see that only the term highlighted with an underbrace can contribute to \bar{V}_5 . Hence, we are led back to Eq. (6.3).

Then, we carry out step (ii). Evidently, only the term $r_\mu \mathbb{B}_2(p, q, r)$ of Eq. (6.6) contributes to the tensor structure $r_\mu p_\nu$. Hence, we can write

$$q^\alpha (e_2)_{\alpha\mu\nu} = -\frac{\lambda Z_3 F(q) \mathbb{B}_2(p, q, r) r_\mu}{p^2} \int_k \Delta^{\rho\delta}(k-p) \Delta^{\sigma\tau}(k) \times \Gamma_{\nu\sigma\rho}^{(0)}(-p, k, p-k) \times [V_1(-p, k, p-k) g_{\delta\tau} + V_2(-p, k, p-k) p_\delta p_\tau] + \dots, \tag{8.15}$$

with the ellipsis denoting terms that cannot contribute to \bar{V}_5 because they do not contain either a $1/p^2$ or a r_μ .

Then, for small p , we can expand Eq. (8.15) around $p = 0$, using Eq. (2.8). Note that to first order in p , Eq. (6.7) implies $\mathbb{B}_2(p, q, r) = -(p \cdot q) \mathbb{A}_3(0, q, -q)$. Hence, we obtain

$$q^\alpha (e_2)_{\alpha\mu\nu} = -F(q)(q \cdot p) q^2 \mathbb{A}_3(0, q, -q) \left(\frac{r_\mu p_\nu}{r^2 p^2} \right) \times \left[3\lambda Z_3 \int_k k^2 \Delta^2(k) \mathbb{C}(k) \right] + \dots, \tag{8.16}$$

with ellipsis now including terms that are dropped in the expansion around $p = 0$.

To complete step (ii), we note that the form factor of the tensor $r_\mu p_\nu$ is $\bar{V}_5/p^2 r^2 + S_5$. Hence, invoking Eq. (2.9),

$$\frac{\bar{V}_5^{(e_2)}}{p^2 r^2} + S_5^{(e_2)} = \frac{\bar{V}_5}{p^2 r^2} + S_5^{(e_2)} = -\frac{(q \cdot p)}{r^2 p^2} F(q) q^2 \mathbb{A}_3(0, q, -q) m_{(a_1)}^2 + \dots \tag{8.17}$$

Note that in the first equality, we used the fact that only (e_2) contributes to \bar{V}_5 , i.e., $\bar{V}_5 = \bar{V}_5^{(e_2)}$, whereas S_5 may receive contributions from other diagrams.

Proceeding to step (iii), we multiply Eq. (8.17) by $r^2 p^2$ and expand the result to the first order in p . Using Eq. (8.10), we find

$$\bar{V}'_5(q) = -\frac{F(q)m_{(a_1)}^2}{2} \left[q^2 A_3(0, q, -q) + A_3^{\mathbf{P}}(0, q, -q) \right]. \tag{8.18}$$

Note that this result is nearly identical to Eq. (8.9), differing from it only by the substitutions $m \rightarrow m_{(a_1)}$ and $A_3^{\mathbf{P}}(q) \rightarrow 0$.

Finally, we perform (iv), i.e., expand Eq. (8.18) around $q = 0$. Using Eq. (5.19), we obtain

$$\bar{V}'_5(q) = q^2 f_3(0), \quad f_3(0) := -\frac{F(0)m_{(a_1)}^2}{2} \left\{ A_3(0, 0, 0) + \left[\frac{dA_3^{\mathbf{P}}(0, q, -q)}{dq^2} \right]_{q=0} \right\}, \tag{8.19}$$

which is Eq. (8.11), with $f(0) := f_3(0)$.

As in the previous section, the STI results given by Eqs. (8.11) and (8.12), and the SDE result in Eq. (8.19) are strikingly similar; again, the observed discrepancy is due to the SDE truncation, or the approximate nature of the STI in Eq. (6.1).

9 Conclusions

The intense scrutiny of the correlation functions of QCD by means of continuous methods [9, 23, 27, 34, 79, 122–124], and lattice simulations [66, 125–130], supports the notion that the gluons acquire a nonperturbative mass [63, 64] through the action of the celebrated Schwinger mechanism. In a non-Abelian context, the main dynamical characteristic of this mechanism is the formation of composite massless poles in the vertices of the theory [15–21]. These poles display the crucial feature of being completely longitudinally coupled, a fact that guarantees the absence of divergences in (Landau gauge) lattice form factors.

In this article we have analyzed the pole content of the three-gluon vertex, whose role is known to be instrumental in the realization of the Schwinger mechanism, accounting for the bulk of the gluon mass [13, 14, 63, 64]. It turns out that the resulting structures are quite rich, being imposed by Bose-symmetry and the STI satisfied by the three-gluon vertex. In particular, we have focused on the appearance and role of the mixed double and triple poles, of the type $1/q^2 p^2$ and $1/q^2 r^2 p^2$, respectively, which are inert as far as the direct act of mass generation is concerned.

It turns out that the mixed double poles are an indispensable requirement for the flawless completion of the STI satisfied by this vertex in the presence of an infrared finite (massive) gluon propagator. In fact, the STI imposes powerful constraints relating the so-called “residue function” to all other components entering in the STI. We emphasize that, at this level, the presence of these poles is dictated solely by the STI, and is not related to any particular dynamical realization. In that sense, it appears to be of general validity, hinging only on the longitudinal nature of the poles. The picture emerging from the bound-state realization of the Schwinger mechanism, as captured by the vertex SDE [22, 24, 43, 44], satisfies the general constraints imposed by the STI, thus passing a highly nontrivial self-consistency check.

As for the mixed triple pole, our analysis reveals that their strength is substantially reduced (i.e., weaker than a double mixed pole), again by virtue of inescapable requirements imposed by the STI. Interestingly enough, the salient qualitative features of this result are recovered by the vertex SDE, exposing once again the complementarity between symmetry and dynamics.

Our analysis strongly indicates that higher n -point functions (i.e., Green’s functions with n incoming gluons, and $n > 3$) will also possess an extended structure of poles. This is already seen at the level of the four-gluon vertex $\Pi_{\alpha\mu\delta\tau}^{abts}$ ($n = 4$), which enters in the demonstration of Sect. 6. In particular, $\Pi_{\alpha\mu\delta\tau}^{abts}$ is forced by the STI of Eq. (6.1), namely

by the V -parts of the three-gluon vertices appearing on the r.h.s., to have poles in all channels carrying the momenta of the external legs, together with the channels obtained by forming sums of momenta, as happens in the case $p = q + r$. A preliminary study reveals that the diagrammatic interpretation of all these poles is fully consistent with the notions and elements introduced in Sect. 3. We hope to report the results of a detailed inquiry in the near future.

It would be clearly important to unravel an organizing principle that accounts for the pole proliferation in the fundamental vertices of QCD. A possible approach is the construction of low-energy effective descriptions of Yang–Mills theories with a gluon mass, in the spirit of the gauged non-linear sigma model proposed by Cornwall, see [21, 99, 100, 131]. In this model, the addition of a gluon mass at the level of the effective Lagrangian is compensated by the presence of angle-valued scalar fields, which act as would-be Nambu–Goldstone particles. When the equation of motion of these scalars is solved as a power series in the gauge field, and the solution is substituted back into the Lagrangian, the various vertices acquire longitudinally coupled massless poles, see, e.g., Eq. (5.4). A systematic comparison between the pole patterns obtained within this model (or variants thereof) and those induced by the Schwinger mechanism at the level of the fundamental theory, as detailed here, might afford clues on the structure of possible low-energy effective descriptions of QCD.

Acknowledgements The work of A. C. A., B. M. O., and L. R. S. is supported by the CNPq grants 307854/2019-1, 141409/2021-5, and 162264/2022-4, respectively. A. C. A. also acknowledges financial support from project 464898/2014-5 (INCT-FNA). M. N. F. and J. P. are supported by the Spanish MICINN grant PID2020-113334GB-I00. M. N. F. acknowledges financial support from Generalitat Valenciana through contract CIAPOS/2021/74. J. P. also acknowledges funding from the regional Prometeo/2019/087 from the Generalitat Valenciana.

Data availability statement This manuscript has no associated data or the data will not be deposited. [Authors’ comment: The datasets generated during and/or analysed during the current study are available from the corresponding author on reasonable request.]

Open Access This article is licensed under a Creative Commons Attribution 4.0 International License, which permits use, sharing, adaptation, distribution and reproduction in any medium or format, as long as you give appropriate credit to the original author(s) and the source, provide a link to the Creative Commons licence, and indicate if changes were made. The images or other third party material in this article are included in the article’s Creative Commons licence, unless indicated otherwise in a credit line to the material. If material is not included in the article’s Creative Commons licence and your intended use is not permitted by statutory regulation or exceeds the permitted use, you will need to obtain permission directly from the copyright holder. To view a copy of this licence, visit <http://creativecommons.org/licenses/by/4.0/>.

Funded by SCOAP³. SCOAP³ supports the goals of the International Year of Basic Sciences for Sustainable Development.

References

1. J.M. Cornwall, Phys. Rev. D **26**, 1453 (1982). <https://doi.org/10.1103/PhysRevD.26.1453>
2. C.W. Bernard, Phys. Lett. B **108**, 431 (1982). [https://doi.org/10.1016/0370-2693\(82\)91228-X](https://doi.org/10.1016/0370-2693(82)91228-X)
3. C.W. Bernard, Nucl. Phys. B **219**, 341 (1983). [https://doi.org/10.1016/0550-3213\(83\)90645-4](https://doi.org/10.1016/0550-3213(83)90645-4)
4. G. Parisi, R. Petronzio, Phys. Lett. B **94**, 51 (1980). [https://doi.org/10.1016/0370-2693\(80\)90822-9](https://doi.org/10.1016/0370-2693(80)90822-9)
5. J.F. Donoghue, Phys. Rev. D **29**, 2559 (1984). <https://doi.org/10.1103/PhysRevD.29.2559>
6. J. Mandula, M. Ogilvie, Phys. Lett. B **185**, 127 (1987). [https://doi.org/10.1016/0370-2693\(87\)91541-3](https://doi.org/10.1016/0370-2693(87)91541-3)
7. J.M. Cornwall, J. Papavassiliou, Phys. Rev. D **40**, 3474 (1989). <https://doi.org/10.1103/PhysRevD.40.3474>
8. K.G. Wilson, T.S. Walhout, A. Harindranath, W.-M. Zhang, R.J. Perry, S.D. Glazek, Phys. Rev. D **49**, 6720 (1994). <https://doi.org/10.1103/PhysRevD.49.6720>
9. A.C. Aguilar, D. Binosi, J. Papavassiliou, Phys. Rev. D **78**, 025010 (2008). <https://doi.org/10.1103/PhysRevD.78.025010>
10. J.S. Schwinger, Phys. Rev. **125**, 397 (1962). <https://doi.org/10.1103/PhysRev.125.397>
11. J.S. Schwinger, Phys. Rev. **128**, 2425 (1962). <https://doi.org/10.1103/PhysRev.128.2425>
12. C.D. Roberts, Symmetry **12**, 1468 (2020). <https://doi.org/10.3390/sym12091468>
13. J. Papavassiliou, Chin. Phys. C **46**, 112001 (2022). <https://doi.org/10.1088/1674-1137/ac84ca>
14. M.N. Ferreira, J. Papavassiliou, Particles **6**, 312 (2023). <https://doi.org/10.3390/particles6010017>
15. R. Jackiw, K. Johnson, Phys. Rev. D **8**, 2386 (1973). <https://doi.org/10.1103/PhysRevD.8.2386>
16. R. Jackiw, *Proceedings, Laws Of Hadronic Matter, Erice* (MIT, Cambridge, 1973)
17. E. Eichten, F. Feinberg, Phys. Rev. D **10**, 3254 (1974). <https://doi.org/10.1103/PhysRevD.10.3254>
18. E.C. Poggio, E. Tomboulis, S.H.H. Tye, Phys. Rev. D **11**, 2839 (1975). <https://doi.org/10.1103/PhysRevD.11.2839>
19. J. Smit, Phys. Rev. D **10**, 2473 (1974). <https://doi.org/10.1103/PhysRevD.10.2473>
20. J. Cornwall, R. Norton, Phys. Rev. D **8**, 3338 (1973). <https://doi.org/10.1103/PhysRevD.8.3338>
21. J.M. Cornwall, Nucl. Phys. B **157**, 392 (1979). [https://doi.org/10.1016/0550-3213\(79\)90111-1](https://doi.org/10.1016/0550-3213(79)90111-1)
22. A.C. Aguilar, D. Ibanez, V. Mathieu, J. Papavassiliou, Phys. Rev. D **85**, 014018 (2012). <https://doi.org/10.1103/PhysRevD.85.014018>
23. D. Binosi, D. Ibañez, J. Papavassiliou, Phys. Rev. D **86**, 085033 (2012). <https://doi.org/10.1103/PhysRevD.86.085033>
24. D. Ibañez, J. Papavassiliou, Phys. Rev. D **87**, 034008 (2013). <https://doi.org/10.1103/PhysRevD.87.034008>
25. K.-I. Kondo, Phys. Lett. B **514**, 335 (2001). [https://doi.org/10.1016/S0370-2693\(01\)00817-6](https://doi.org/10.1016/S0370-2693(01)00817-6)
26. J. Braun, H. Gies, J.M. Pawłowski, Phys. Lett. B **684**, 262 (2010). <https://doi.org/10.1016/j.physletb.2010.01.009>
27. C.S. Fischer, A. Maas, J.M. Pawłowski, Ann. Phys. **324**, 2408 (2009). <https://doi.org/10.1016/j.aop.2009.07.009>
28. D.R. Campagnari, H. Reinhardt, Phys. Rev. D **82**, 105021 (2010). <https://doi.org/10.1103/PhysRevD.82.105021>
29. M. Tissier, N. Wschebor, Phys. Rev. D **82**, 101701 (2010). <https://doi.org/10.1103/PhysRevD.82.101701>
30. J. Serreau, M. Tissier, Phys. Lett. B **712**, 97 (2012). <https://doi.org/10.1016/j.physletb.2012.04.041>
31. M. Peláez, M. Tissier, N. Wschebor, Phys. Rev. D **90**, 065031 (2014). <https://doi.org/10.1103/PhysRevD.90.065031>
32. F. Siringo, Nucl. Phys. B **907**, 572 (2016). <https://doi.org/10.1016/j.nuclphysb.2016.04.028>
33. G. Eichmann, J.M. Pawłowski, Ja.M. Silva, Phys. Rev. D **104**, 114016 (2021). <https://doi.org/10.1103/PhysRevD.104.114016>
34. J. Horak, F. Ihssen, J. Papavassiliou, J.M. Pawłowski, A. Weber, C. Wetterich, SciPost Phys. **13**, 042 (2022). <https://doi.org/10.21468/SciPostPhys.13.2.042>
35. C.D. Roberts, A.G. Williams, Prog. Part. Nucl. Phys. **33**, 477 (1994). [https://doi.org/10.1016/0146-6410\(94\)90049-3](https://doi.org/10.1016/0146-6410(94)90049-3)
36. R. Alkofer, L. von Smekal, Phys. Rep. **353**, 281 (2001). [https://doi.org/10.1016/S0370-1573\(01\)00010-2](https://doi.org/10.1016/S0370-1573(01)00010-2)
37. C.S. Fischer, J. Phys. G **32**, R253 (2006). <https://doi.org/10.1088/0954-3899/32/8/R02>
38. C.D. Roberts, Prog. Part. Nucl. Phys. **61**, 50 (2008). <https://doi.org/10.1016/j.pnpnp.2007.12.034>
39. D. Binosi, J. Papavassiliou, Phys. Rep. **479**, 1 (2009). <https://doi.org/10.1016/j.physrep.2009.05.001>
40. I.C. Cloet, C.D. Roberts, Prog. Part. Nucl. Phys. **77**, 1 (2014). <https://doi.org/10.1016/j.pnpnp.2014.02.001>
41. A.C. Aguilar, D. Binosi, J. Papavassiliou, Front. Phys. (Beijing) **11**, 111203 (2016). <https://doi.org/10.1007/s11467-015-0517-6>
42. M.Q. Huber, Phys. Rep. **879**, 1 (2020). <https://doi.org/10.1016/j.physrep.2020.04.004>
43. A.C. Aguilar, D. Binosi, C.T. Figueiredo, J. Papavassiliou, Eur. Phys. J. C **78**, 181 (2018). <https://doi.org/10.1140/epjc/s10052-018-5679-2>
44. D. Binosi, J. Papavassiliou, Phys. Rev. D **97**, 054029 (2018). <https://doi.org/10.1103/PhysRevD.97.054029>
45. C. Parrinello, Phys. Rev. D **50**, R4247 (1994). <https://doi.org/10.1103/PhysRevD.50.R4247>
46. B. Alles, D. Henty, H. Panagopoulos, C. Parrinello, C. Pittori, D.G. Richards, Nucl. Phys. B **502**, 325 (1997). [https://doi.org/10.1016/S0550-3213\(97\)00483-5](https://doi.org/10.1016/S0550-3213(97)00483-5)
47. C. Parrinello, D. Richards, B. Alles, H. Panagopoulos, C. Pittori, (UKQCD), Nucl. Phys. B Proc. Suppl. **63**, 245 (1998). [https://doi.org/10.1016/S0920-5632\(97\)00734-2](https://doi.org/10.1016/S0920-5632(97)00734-2)
48. P. Boucaud, J.P. Leroy, J. Micheli, O. Pene, C. Roiesnel, J. High Energy Phys. **10**, 017 (1998). <https://doi.org/10.1088/1126-6708/1998/10/017>
49. A. Cucchieri, A. Maas, T. Mendes, Phys. Rev. D **74**, 014503 (2006). <https://doi.org/10.1103/PhysRevD.74.014503>
50. A. Maas, Phys. Rev. D **75**, 116004 (2007). <https://doi.org/10.1103/PhysRevD.75.116004>
51. A. Cucchieri, A. Maas, T. Mendes, Phys. Rev. D **77**, 094510 (2008). <https://doi.org/10.1103/PhysRevD.77.094510>
52. A. Athenodorou, D. Binosi, P. Boucaud, F. De Soto, J. Papavassiliou, J. Rodríguez-Quintero, S. Zafeiropoulos, Phys. Lett. B **761**, 444 (2016). <https://doi.org/10.1016/j.physletb.2016.08.065>
53. A.G. Duarte, O. Oliveira, P.J. Silva, Phys. Rev. D **94**, 074502 (2016). <https://doi.org/10.1103/PhysRevD.94.074502>
54. P. Boucaud, F. De Soto, J. Rodríguez-Quintero, S. Zafeiropoulos, Phys. Rev. D **95**, 114503 (2017). <https://doi.org/10.1103/PhysRevD.95.114503>
55. A. Sternbeck, P.-H. Balduf, A. Kizilersu, O. Oliveira, P.J. Silva, J.-I. Skullerud, A.G. Williams, PoS LATTICE2016, 349 (2017). <https://doi.org/10.22323/1.256.0349>
56. M. Vujanovic, T. Mendes, Phys. Rev. D **99**, 034501 (2019). <https://doi.org/10.1103/PhysRevD.99.034501>
57. P. Boucaud, F. De Soto, K. Raya, J. Rodríguez-Quintero, S. Zafeiropoulos, Phys. Rev. D **98**, 114515 (2018). <https://doi.org/10.1103/PhysRevD.98.114515>
58. A.C. Aguilar, F. De Soto, M.N. Ferreira, J. Papavassiliou, J. Rodríguez-Quintero, S. Zafeiropoulos, Eur. Phys. J. C **80**, 154 (2020). <https://doi.org/10.1140/epjc/s10052-020-7741-0>

59. A.C. Aguilar, F. De Soto, M.N. Ferreira, J. Papavassiliou, J. Rodríguez-Quintero, Phys. Lett. B **818**, 136352 (2021). <https://doi.org/10.1016/j.physletb.2021.136352>
60. F. Pinto-Gómez, F. De Soto, M.N. Ferreira, J. Papavassiliou, J. Rodríguez-Quintero, Phys. Lett. B **838**, 137737 (2023). <https://doi.org/10.1016/j.physletb.2023.137737>
61. G.T.R. Catumba, O. Oliveira, P.J. Silva, PoS **LATTICE2021**, 467 (2022). <https://doi.org/10.22323/1.396.0467>
62. G.T.R. Catumba, O. Oliveira, P.J. Silva, EPJ Web Conf. **258**, 02008 (2022). <https://doi.org/10.1051/epjconf/202225802008>
63. A.C. Aguilar, M.N. Ferreira, J. Papavassiliou, Phys. Rev. D **105**, 014030 (2022). <https://doi.org/10.1103/PhysRevD.105.014030>
64. A.C. Aguilar, F. De Soto, M.N. Ferreira, J. Papavassiliou, F. Pinto-Gómez, C.D. Roberts, J. Rodríguez-Quintero, Phys. Lett. B **841**, 137906 (2023). <https://doi.org/10.1016/j.physletb.2023.137906>
65. M. Narciso Ferreira, Few Body Syst. **64**, 27 (2023). <https://doi.org/10.1007/s00601-023-01813-0>
66. I. Bogolubsky, E. Ilgenfritz, M. Muller-Preussker, A. Sternbeck, Phys. Lett. B **676**, 69 (2009). <https://doi.org/10.1016/j.physletb.2009.04.076>
67. A.C. Aguilar, C.O. Ambrósio, F. De Soto, M.N. Ferreira, B.M. Oliveira, J. Papavassiliou, J. Rodríguez-Quintero, Phys. Rev. D **104**, 054028 (2021). <https://doi.org/10.1103/PhysRevD.104.054028>
68. C. Becchi, A. Rouet, R. Stora, Ann. Phys. **98**, 287 (1976). [https://doi.org/10.1016/0003-4916\(76\)90156-1](https://doi.org/10.1016/0003-4916(76)90156-1)
69. I.V. Tyutin, preprint of P.N. Lebedev Physical Institute, LEBEDEV-75-39 (1975). <https://doi.org/10.48550/arXiv.0812.0580>
70. J. Taylor, Nucl. Phys. B **33**, 436 (1971). [https://doi.org/10.1016/0550-3213\(71\)90297-5](https://doi.org/10.1016/0550-3213(71)90297-5)
71. A. Slavnov, Theor. Math. Phys. **10**, 99 (1972). <https://doi.org/10.1007/BF01090719>
72. W.J. Marciano, H. Pagels, Phys. Rep. **36**, 137 (1978). [https://doi.org/10.1016/0370-1573\(78\)90208-9](https://doi.org/10.1016/0370-1573(78)90208-9)
73. J.S. Ball, T.-W. Chiu, Phys. Rev. D **22**, 2550 (1980). <https://doi.org/10.1103/PhysRevD.22.2550> [Erratum: Phys. Rev. D 23, 3085 (1981)]
74. A.I. Davydychev, P. Osland, O. Tarasov, Phys. Rev. D **54**, 4087 (1996). <https://doi.org/10.1103/PhysRevD.59.109901> [Erratum: Phys. Rev. D 59, 109901 (1999)]
75. J. Gracey, H. Kibler, D. Kreimer, Phys. Rev. D **100**, 085001 (2019). <https://doi.org/10.1103/PhysRevD.100.085001>
76. A.C. Aguilar, J. Papavassiliou, J. High Energy Phys. **12**, 012 (2006). <https://doi.org/10.1088/1126-6708/2006/12/012>
77. E.E. Salpeter, H.A. Bethe, Phys. Rev. **84**, 1232 (1951). <https://doi.org/10.1103/PhysRev.84.1232>
78. N. Nakanishi, Prog. Theor. Phys. Suppl. **43**, 1 (1969). <https://doi.org/10.1143/PTPS.43.1>
79. A.C. Aguilar, D. Binosi, C.T. Figueiredo, J. Papavassiliou, Phys. Rev. D **94**, 045002 (2016). <https://doi.org/10.1103/PhysRevD.94.045002>
80. D. Binosi, C. Mezrag, J. Papavassiliou, C.D. Roberts, J. Rodríguez-Quintero, Phys. Rev. D **96**, 054026 (2017). <https://doi.org/10.1103/PhysRevD.96.054026>
81. Z.-F. Cui, J.-L. Zhang, D. Binosi, F. de Soto, C. Mezrag, J. Papavassiliou, C.D. Roberts, J. Rodríguez-Quintero, J. Segovia, S. Zafeiropoulos, Chin. Phys. C **44**, 083102 (2020). <https://doi.org/10.1088/1674-1137/44/8/083102>
82. J. Berges, Phys. Rev. D **70**, 105010 (2004). <https://doi.org/10.1103/PhysRevD.70.105010>
83. M.E. Carrington, Y. Guo, Phys. Rev. D **83**, 016006 (2011). <https://doi.org/10.1103/PhysRevD.83.016006>
84. M.C.A. York, G.D. Moore, M. Tassler, JHEP **06**, 077 (2012). [https://doi.org/10.1007/JHEP06\(2012\)077](https://doi.org/10.1007/JHEP06(2012)077)
85. M.E. Carrington, W. Fu, T. Fugleberg, D. Pickering, I. Russell, Phys. Rev. D **88**, 085024 (2013). <https://doi.org/10.1103/PhysRevD.88.085024>
86. R. Williams, C.S. Fischer, W. Heupel, Phys. Rev. D **93**, 034026 (2016). <https://doi.org/10.1103/PhysRevD.93.034026>
87. M.Q. Huber, Phys. Rev. D **101**, 114009 (2020). <https://doi.org/10.1103/PhysRevD.101.114009>
88. A. Maas, M. Vujanović, SciPost Phys. Core **5**, 019 (2022). <https://doi.org/10.21468/SciPostPhysCore.5.2.019>
89. F. Pinto-Gómez, F. De Soto, M.N. Ferreira, J. Papavassiliou, J. Rodríguez-Quintero, (HSV), PoS **LATTICE2022**, 382 (2023). <https://doi.org/10.22323/1.430.0382>
90. A.C. Aguilar, M.N. Ferreira, C.T. Figueiredo, J. Papavassiliou, Phys. Rev. D **99**, 094010 (2019). <https://doi.org/10.1103/PhysRevD.99.094010>
91. G. Eichmann, R. Williams, R. Alkofer, M. Vujanovic, Phys. Rev. D **89**, 105014 (2014). <https://doi.org/10.1103/PhysRevD.89.105014>
92. D. Dudal, J.A. Gracey, S.P. Sorella, N. Vandersickel, H. Verschelde, Phys. Rev. D **78**, 065047 (2008). <https://doi.org/10.1103/PhysRevD.78.065047>
93. M.A.L. Capri, D. Fiorentini, M.S. Guimaraes, B.W. Mintz, L.F. Palhares, S.P. Sorella, D. Dudal, I.F. Justo, A.D. Pereira, R.F. Sobreiro, Phys. Rev. D **92**, 045039 (2015). <https://doi.org/10.1103/PhysRevD.92.045039>
94. T. Kugo, I. Ojima, Prog. Theor. Phys. Suppl. **66**, 1 (1979). <https://doi.org/10.1143/PTPS.66.1>
95. N. Alkofer, R. Alkofer, PoS **FACESQCD**, 043 (2010). <https://doi.org/10.22323/1.117.0043>
96. N. Alkofer, R. Alkofer, Phys. Lett. B **702**, 158 (2011). <https://doi.org/10.1016/j.physletb.2011.06.073>
97. A.K. Cyrol, L. Fister, M. Mitter, J.M. Pawłowski, N. Strodthoff, Phys. Rev. D **94**, 054005 (2016). <https://doi.org/10.1103/PhysRevD.94.054005>
98. J.M. Pawłowski, C.S. Schneider, N. Wink, [arXiv:2202.11123](https://arxiv.org/abs/2202.11123) [hep-th]
99. J.M. Cornwall, W.-S. Hou, Phys. Rev. D **34**, 585 (1986). <https://doi.org/10.1103/PhysRevD.34.585>
100. J.M. Cornwall, J. Papavassiliou, D. Binosi, *The Pinch Technique and its Applications to Non-Abelian Gauge Theories*, vol. 31 (Cambridge University Press, Cambridge, 2010)
101. A.C. Aguilar, M.N. Ferreira, C.T. Figueiredo, J. Papavassiliou, Phys. Rev. D **99**, 034026 (2019). <https://doi.org/10.1103/PhysRevD.99.034026>
102. A.C. Aguilar, M.N. Ferreira, J. Papavassiliou, Eur. Phys. J. C **80**, 887 (2020). <https://doi.org/10.1140/epjc/s10052-020-08453-2>
103. P. Pascual, R. Tarrach, Nucl. Phys. B **174**, 123 (1980). [https://doi.org/10.1016/0550-3213\(80\)90193-5](https://doi.org/10.1016/0550-3213(80)90193-5) [Erratum: Nucl. Phys. B 181, 546 (1981)]
104. J. Papavassiliou, Phys. Rev. D **47**, 4728 (1993). <https://doi.org/10.1103/PhysRevD.47.4728>
105. S. Hashimoto, J. Kodaira, Y. Yasui, K. Sasaki, Phys. Rev. D **50**, 7066 (1994). <https://doi.org/10.1103/PhysRevD.50.7066>
106. L. Driesen, M. Stingl, Eur. Phys. J. A **4**, 401 (1999). <https://doi.org/10.1007/s100500050247>
107. C. Kellermann, C.S. Fischer, Phys. Rev. D **78**, 025015 (2008). <https://doi.org/10.1103/PhysRevD.78.025015>
108. N. Ahmadiaz, C. Schubert, PoS **QCD-TNT-III**, 002 (2013). <https://doi.org/10.22323/1.193.0002>
109. J.A. Gracey, Phys. Rev. D **90**, 025011 (2014). <https://doi.org/10.1103/PhysRevD.90.025011>
110. A.K. Cyrol, M.Q. Huber, L. von Smekal, Eur. Phys. J. C **75**, 102 (2015). <https://doi.org/10.1140/epjc/s10052-015-3312-1>
111. D. Binosi, D. Ibañez, J. Papavassiliou, J. High Energy Phys. **09**, 059 (2014). [https://doi.org/10.1007/JHEP09\(2014\)059](https://doi.org/10.1007/JHEP09(2014)059)

112. G. Eichmann, C.S. Fischer, W. Heupel, Phys. Rev. D **92**, 056006 (2015). <https://doi.org/10.1103/PhysRevD.92.056006>
113. J.A. Gracey, Phys. Rev. D **95**, 065013 (2017). <https://doi.org/10.1103/PhysRevD.95.065013>
114. M. Baker, C.-K. Lee, Phys. Rev. D **15**, 2201 (1977). <https://doi.org/10.1103/PhysRevD.17.2182> [Erratum: Phys. Rev. D 17, 2182 (1978)]
115. S.K. Kim, M. Baker, Nucl. Phys. B **164**, 152 (1980). [https://doi.org/10.1016/0550-3213\(80\)90506-4](https://doi.org/10.1016/0550-3213(80)90506-4)
116. A.C. Aguilar, D. Binosi, J. Papavassiliou, J. Rodriguez-Quintero, Phys. Rev. D **80**, 085018 (2009). <https://doi.org/10.1103/PhysRevD.80.085018>
117. L. von Smekal, K. Maltman, A. Sternbeck, Phys. Lett. B **681**, 336 (2009). <https://doi.org/10.1016/j.physletb.2009.10.030>
118. P. Boucaud, F. De Soto, J. Leroy, A. Le Yaouanc, J. Micheli et al., Phys. Rev. D **79**, 014508 (2009). <https://doi.org/10.1103/PhysRevD.79.014508>
119. P. Boucaud, D. Dudal, J. Leroy, O. Pene, J. Rodriguez-Quintero, J. High Energy Phys. **12**, 018 (2011). [https://doi.org/10.1007/JHEP12\(2011\)018](https://doi.org/10.1007/JHEP12(2011)018)
120. S. Zafeiropoulos, P. Boucaud, F. De Soto, J. Rodríguez-Quintero, J. Segovia, Phys. Rev. Lett. **122**, 162002 (2019). <https://doi.org/10.1103/PhysRevLett.122.162002>
121. W.H. Press, S.A. Teukolsky, W.T. Vetterling, B.P. Flannery, *Numerical Recipes in FORTRAN: The Art of Scientific Computing* (Cambridge University Press, Cambridge, 1992)
122. J. Rodriguez-Quintero, J. High Energy Phys. **01**, 105 (2011). [https://doi.org/10.1007/JHEP01\(2011\)105](https://doi.org/10.1007/JHEP01(2011)105)
123. A.C. Aguilar, A.A. Natale, P.S. Rodrigues da Silva, Phys. Rev. Lett. **90**, 152001 (2003). <https://doi.org/10.1103/PhysRevLett.90.152001>
124. A.C. Aguilar, A.A. Natale, J. High Energy Phys. **08**, 057 (2004). <https://doi.org/10.1088/1126-6708/2004/08/057>
125. A. Cucchieri, T. Mendes, PoS **LATTICE2007**, 297 (2007). <https://doi.org/10.22323/1.042.0297>
126. A. Cucchieri, T. Mendes, Phys. Rev. Lett. **100**, 241601 (2008). <https://doi.org/10.1103/PhysRevLett.100.241601>
127. I. Bogolubsky, E. Ilgenfritz, M. Muller-Preussker, A. Sternbeck, PoS **LATTICE2007**, 290 (2007). <https://doi.org/10.22323/1.042.0290>
128. O. Oliveira, P. Silva, PoS **LAT2009**, 226 (2009). <https://doi.org/10.22323/1.091.0226>
129. O. Oliveira, P. Bicudo, J. Phys. G **G38**, 045003 (2011). <https://doi.org/10.1088/0954-3899/38/4/045003>
130. A. Cucchieri, T. Mendes, Phys. Rev. D **81**, 016005 (2010). <https://doi.org/10.1103/PhysRevD.81.016005>
131. J.M. Cornwall, Phys. Rev. D **10**, 500 (1974). <https://doi.org/10.1103/PhysRevD.10.500>